Epigenetic signature of human immune aging: the GESTALT study

Roshni Roy[1], Pei-Lun Kuo[2], Julián Candia[2], Dimitra Sarantopoulou[1], Ceereena Ubaida-Mohien[2], Dena Hernandez[3], Mary Kaileh[1], Sampath Arepalli[3], Amit Singh[1], Arsun Bektas[2], Jaekwan Kim[1], Ann Zenobia Moore[2], Toshiko Tanaka[2], Julia McKelvey[4], Linda Zukley[4], Cuong Nguyen[5], Tonya Wallace[5], Christopher Dunn[5], William Wood[6], Yulan Piao[6], Christopher Coletta[6], Supriyo De[6], Jyoti Misra Sen[7], Nan-ping Weng[1], Ranjan Sen[1], Luigi Ferrucci[3]*

[1] Laboratory of Molecular Biology and Immunology
[2] Translational Gerontology Branch
[3] Laboratory of Neurogenetics
[4] Clinical Research Core
[5] Flow Cytometry Unit
[6] Laboratory of Genetics & Genomics
[7] Laboratory of Clinical Investigation
National Institute on Aging, Baltimore, MD

* - Corresponding and lead author (correspondence- ferruccilu@grc.nia.nih.gov)

ABSTRACT

Age-associated DNA methylation in blood cells convey information on health status. However, the mechanisms that drive these changes in circulating cells and their relationships to gene regulation are unknown. We identified age-associated DNA methylation sites in six purified blood borne immune cell types (naïve B, naïve $CD4^+$ and $CD8^+$ T cells, granulocytes, monocytes and NK cells) collected from healthy individuals interspersed over a wide age range. Of the thousand of age-associated sites, only 350 sites were differentially methylated in the same direction in all cell types and validated in an independent longitudinal cohort. Genes close to age-associated hypomethylated sites were enriched for collagen biosynthesis and complement cascade pathways, while genes close to hypermethylated sites mapped to neuronal pathways. In-silico analyses showed that in most cell types, the age-associated hypo- and hypermethylated sites were enriched for ARNT (HIF1β) and REST transcription factor motifs respectively, which are both master regulators of hypoxia response. To conclude, despite spatial heterogeneity, there is a commonality in the putative regulatory role with respect to transcription factor motifs and histone modifications at and around these sites. These features suggest that DNA methylation changes in healthy aging may be adaptive responses to fluctuations of oxygen availability.

Keywords- DNA methylation, immune cells, aging, ARNT, REST, hypoxia

INTRODUCTION

Human aging is associated with site-specific changes of DNA methylation. Summary measures of DNA methylation called “epigenetic clocks” are extensively used in aging research to estimate biological aging(1-3). Epigenetic clocks closely approximate chronological age and beyond age, predict adverse health conditions, including frailty (4), Alzheimer’s disease (5) and mortality(6, 7).

Research suggest that changes in DNA methylation with aging are regulated by specific mechanisms rather than by a stochastic drift (8). For example, a loss-of-function mutation in the H3K36 histone methyltransferase has been associated with epigenetic aging in mice (9). In humans, polymorphisms in the telomerase gene (TERT) (10) and age-dependent gain of methylation in the Polycomb repressive complex 2 have been related to accelerated aging(11). However, so far, no sound hypothesis exists that explains the association of DNA methylation with aging and pathology.

A main obstacle in understanding mechanisms driving age-associated changes of DNA methylation is that most human studies were performed in mixed blood cell types. The few studies that investigated select immune circulating cells failed to propose a unifying biological hypothesis explaining predictable changes of DNA methylation with aging(12-18).

We analyzed age-associated methylation in 6 purified blood-borne cell types sorted from peripheral mononuclear cells (PBMCs) from individuals of different ages. To minimize the confounding of age-associated pre-clinical and clinical diseases, participants were ascertained to be healthy by trained health professionals according to strict clinical

criteria. We looked for CpGs differentially methylated with aging in the same direction in multiple cell types. Next, in each cell type, we conducted enrichment analyses of genes close to age-associated CpGs. Finally, we looked for chromatin accessibility markers and transcription factor binding sites close to the same age-associated CpGs. Our findings suggest that changes in methylation with aging are related to fluctuation of energetic metabolism during the life course.

RESULTS

Age-associated methylation in individual cell types

A principal component analysis on normalized DNA methylation (Figure 1A and Supplementary Table 1) showed that clustering by cell types was stronger than by age (PC2 showed cell types-based clustering- 11.3 %) (Supplementary Fig. 1A).

Age-associated CpGs were identified through sex-adjusted beta regression models (FDR corrected p-value <0.05). Number of hypo- or hypermethylated sites varied considerably between cell types (Figure 1B) with highest numbers in $CD4^+$ T cells (Supplementary Fig. 1B and Supplementary Table 2). Using a different approach of comparing between young ($\leq$35 years, 25th percentile) and old ($\geq$70 years, 75th percentile) individuals, we observed >90% overlap with beta regression-derived hypomethylated sites and 70-95% overlap with hypermethylated sites in all cell types except $CD8^+$ T cells (9-14% overlap) (Supplementary Fig. 1C). Having fewer old donors with $CD8^+$ T cells may have contributed to differences (Supplementary Table 1).

Similar to other studies, we found that a significant proportion of age-hypomethylated CpGs were in the intergenic and open-sea (>4kb from CpG island) regions while age-

hypermethylated CpGs were in promoters and CpG islands (Chi sq test $p<0.001$) (Supplementary Figs. 1D and 1E). Additionally, age-associated differentially methylated sites in PBMC poorly recapitulate age-dependent changes that take place in specific primary immune cells (Supplementary Figs. 1E-F). These findings point to a wide heterogeneity of age-differential CpG methylation across immune blood cells and suggest that studies in PBMC poorly represents the changes that take place in specific cell types with aging.

Shared age associated methylation across cell types

Only 181 age-associated hypomethylated sites and 169 hypermethylated sites were shared between all 6 cell types. These numbers increased to 776 (age-hypomethylated) and 404 (age-hypermethylated) sites in 5 or more cell types (Figures 1C-D). Thus, most age-related methylation changes are cell-specific. Of note, only 10 of the sites overlap with the 359 CpGs in Horvath's pan-tissue epigenetic clock (19). While the number of shared age-hypo or hypermethylated CpGs across cells was relatively small, it was highly significantly higher than that expected based on chance alone, suggesting that common underlying epigenetic mechanisms exist across the considered cell types (Figure 1C & D). For example, CpG sites adjacent to *RCAN1* (calcineurin 1) and *KLF14* (Krueppel-Like Factor 14) show similar age-associated patterns in all cell types (Figure 1E and F).

Next, we tested whether the top 15 genes annotated to the most significant age-associated CpGs were common across multiple cell types (Figure 2A-B and Supplementary Figs. 2A-E). Only the age-hypomethylation of *CCDC102B* was common to all cell types (Supplementary Tables 3 and 4) while *ELOVL2*, *GPR78*, *LHFPL4* and *KLF14* were commonly age-hypermethylated in all cell types (Supplementary Tables 3

and 4). These findings suggest that most CpGs with age-associated methylation consistent across cell types undergo moderate (although significant) methylation changes with aging.

Longitudinal validation of age-associated CpG sites

We hypothesized that the age-associated CpGs identified across the six immune cells in this cross-sectional study would also show longitudinal changes of the size and direction predicted. We used DNA methylation data (Illumina 450K microarray on DNA from buffy coats) assessed at baseline and 9- and 13-year follow-up in 699 participants of the InCHIANTI study (20). Of the 181 hypo-methylated and 169 hypermethylated CpGs with age in all cell types in GESTALT, 72 and 135, respectively, were represented in the 450K microarray. The beta-coefficients for age of the 207 CpG probes (72+135) estimated from the GESTALT study and their corresponding values estimated longitudinally from the InCHIANTI study were highly and significantly correlated (hypomethylated with age CpGs: r=0.49, p=1.2e-09 and hypermethylated with age CpGs: r=0.5, p=6.9e-06 for average beta coefficients across 6 cell types, Figures 2C-D and Supplementary Figs. 3A-B). Thus, CpGs identified as differentially methylated with aging across cell types in GESTALT also change longitudinally with aging.

Age-associated probes with opposite trends in different immune cells

Several CpGs showed significant but opposing age-trends in different cell types, especially in B, $CD4^+$ T cells and monocytes (Supplementary Figs. 2F and G). For example, cg27123256 in the gene body of *BCL11B* was age-hypomethylated in non-T cells and significantly age-hypermethylated in naïve $CD4^+$ T cells (Figure 2E). Our

observations implicate BCL11B in aging-related changes in naïve $CD4^+$ T cell function, distinct from its proposed role in effector cells (14, 21, 22). Conversely, cg03530364 in the body of FAM19A1 gene was hypermethylated in non-T cells but age-hypomethylated in $CD4^+$ T cells (Figure 2F). Of note, none of these CpGs were differentially age-methylated in PBMC. Thus, opposite age-methylation trends in specific cell types may cancel each other and obscure their relevance for aging when mixed cell type sample are assessed.

Pathway analysis of age-associated genes

Gene set enrichment analyses were performed on genes associated with at least one CpG significantly age-hypo or hypermethylated in 5 or more cell types. We identified 30 pathways (q-value<0.05) (Figure 3 and Supplementary Table 5). Probes commonly age-hypomethylated in 5 or more cell types (n=776) pointed to genes enriched in collagen biosynthesis, complement cascade and GTPase pathways (left-most column in bottom panel of Figure 3) that highlighted inflammatory and metabolic pathway in aging. Genes associated with shared age-hypermethylated probes (n=404) were enriched for neural pathways previously implicated to brain aging along with G-Protein Coupled Receptors pathways (23) (left-most column in top panel of Figure 3). Key pathways are highlighted, with associated genes displayed in boxes on the right-hand side.

Functional annotation of age-associated probes

To further interrogate the relationships between DNA methylation and other epigenetic states, we mapped the methylation age-associated sites to cell-specific chromHMM-derived chromatin profiles(24). As controls, we annotated all sites in the EPIC array to the

18-state chromHMM model of respective primary cell type. Granulocytes were excluded from this analysis because reference data were not available.

Age-associated hypomethylated CpGs were significantly enriched for weak/active enhancers (yellow bar, Figure 4A) whereas, confirming previous reports, age-hypermethylated CpGs, were enriched in bivalent/polycomb regions compared to control set (brown and dark grey bars respectively in Figure 4A). Results for cell types-specific analyses are shown in Figure 4B.

We further mapped the profile of four epigenetic markers from the ENCODE project in and around (± 3kb) age-associated methylation sites. For B and $CD4^+$ T cells, we observed a V-shaped peak-valley-peak pattern of DNase hypersensitivity at sites of age-associated hypomethylation, which is characteristic of promoter sites (Figure 4C) (25). Both age-associated hypo- and hypermethylated sites showed evident H3K4me1 peaks, a marker commonly associated with active and primed enhancers (Figure 4C)(26). No specific trend was observed for H3K4me3 and H3K27ac (data not shown). These patterns were highly consistent across cell types (Supplementary Fig. 4) and strongly suggest functional connections between methylation and chromatin status.

Pattern of transcription factor binding motifs around age-associated CpGs.

Specific transcription factors (TF) may induce or been induced by DNA methylation (27, 28). Through our *de-novo* HOMER analysis, we observed that the binding motif for aryl hydrocarbon receptor nuclear translocator (*ARNT,* also named HIF1β) was associated with age-hypomethylated CpGs across most cell types (Figure 5A). The only exception was naïve $CD8^+$ T cells where the top enriched motif was B-cell lymphoma gene 6 (*BCL6*).

BCL6 code for a zinc finger transcription factor that plays a critical role in the generation of memory and effector cells in acute infection (29). Another motif associated with age-hypomethylated CpGs across most cell types was chromatin architectural protein CTCF and its closely related gene BORIS. Methylation changes at CTCF sites reflected large scale genome reorganization in immune cells in older individuals (30, 31).

Repressor Element 1-Silencing Transcription Factor (*REST*) was the TF motifs most frequently associated with age-hypermethylated CpGs in 5 of 6 cell types (Figure 5B). Age-hypermethylated sites in PBMCs have been previously shown to be enriched for *REST*, which is known to repress stress response genes and is lost in cognitive impairment and Alzheimer's disease pathology (32, 33). The top enriched TF motif associated with age-hypermethylated sites in monocytes was Arid5A ($p<10^{-27}$) that binds to selective inflammation-related genes, such as *IL6* and *STAT3* and stabilize their expression (34, 35).

The recurring enrichment of *ARNT* and *REST* with age-associated CpGs observed across multiple cell types, despite relatively few shared genomic region locations, suggests this relationship is functional. We found that only 17 and 44 age-associated hypo- and hypermethylated probes, respectively, shared *ARNT* or *REST* motifs across all cells (Supplementary Figs. 5A-B), suggesting these overlaps are not random and have a specific function (Supplementary Figs. 5A and B).

Remarkably, *ARNT* was significantly overexpressed in older age in three of the six cell types and REST showed a significant decrease of expression with age in most cell types (Supplementary Table 6). These findings suggest that age-associated changes in

expression levels of *REST* and *ARNT* can affect the epigenetic status of their target genes.

Age-related differential methylation and oxygen sensing.

ARNT, *REST* and *BCL6*, three transcription factors most associated with differentially methylated regions, are implicated in hypoxia response (Figure 5C). *ARNT* is the beta subunit of Hypoxia Factor 1 (HIF-1), which is stabilized during hypoxia and shuttled to the nucleus where it binds to DNA hypoxia response elements (HRE) and triggers a complex response that include upregulation of angiogenesis and erythropoiesis and reprogramming of energetic metabolism from oxidative phosphorylation to anaerobic glycolysis (36). Hypoxia also upregulates the transcription of *REST* which is the master regulator of the transcriptional repression arm of the response to hypoxia. Released REST is shuttled to the nucleus where it binds to DNA and regulates approximately 20% of the hypoxia-repressed genes, including genes involved in proliferation, translation, and cell cycle progression. We identified 35 genes that were hypomethylated with aging and had close by an ARNT motif in all six cell types (Data not shown). Ten of these genes (right side of Figure 5C, genes under orange headings) have been linked to hypoxia response (37-46). Similarly, we found 20 genes with probes hypermethylated with age and with REST motif in the vicinity in all six cell types (data not shown). Four of these (right side of Figure 5C, genes under green heading) are known to be downregulated in hypoxia (47-50). These results strongly suggest a link between age-associated DNA methylation and oxygen sensing through putative regulation by transcription factors like *ARNT* and *REST* in the various immune cells.

DISCUSSION

Novel and important conclusions arise from our observations. First, only few CpG sites are hypomethylated and hypermethylated with aging across all circulating cells while the majority of significant age-associated methylation changes are cell-selective. Indeed, several CpGs show differential age-methylation in opposite directions in different cell types and are unchanged in PBMC, suggesting that they may be missed when studying mixed cell samples. Noteworthy, age-related methylation differences in this cross-sectional study were strongly and significantly correlated with longitudinal age-associated methylation changes in an independent population.

Age-associated hypomethylated sites were significantly enriched for active enhancers whereas age-hypermethylated sites were enriched for bivalent/polycomb regions, confirming previous findings in whole blood(32). Age-differential methylation coincided with specific chromatin status and histone markers patterns, suggesting that their position in proximity of promoter and active enhancer regions is connected with chromatic accessibility and potentially modulation of gene expression.

Third, distinct TF binding motifs co-localize with CpGs differentially methylated with aging despite wide variation in the distribution of such sites across cell types, suggesting a specific regulatory function. Noteworthy, the top age-associated TF identified, *ARNT* and *REST* act in coordination in hypoxia response (51). *BCL6*, another top TF binding motif associated with age-differentially methylated CpG has also been shown to protects cardiomyocyte from damage during hypoxia (52). These finding supports the hypothesis that systematic methylation changes with aging may be induced by fluctuations in oxygen availability and energy metabolism. Interestingly, the mRNA encoding *ARNT* significantly increases with age in all cell types except monocytes, while mRNA coding for *REST*

declines with aging in 4 cell types and shows no significant change in naïve CD8+ T cells and NK cells. mRNAs coding for *CTCF* showed strong age-association across numerous cell types (Supplementary Table 6). The hypothesis that oxygen sensing regulates directly or indirectly DNA methylations is consistent with studies showing that in replicating fibroblasts, biological age estimated by DNA methylation slows down under hypoxia compared to normoxia(53). Further, many genes close by to “shared” age-differentially methylated CpG identified in our analyses play important roles in hypoxia response (Figure 5C).

The specific mechanisms connecting age-related changes in DNA methylation in genes which also contain binding motifs the master hypoxia-response mediators remain unknown. Shahrzad al. reported an inverse correlation between the severity of hypoxia and the degree of DNA methylation(54). There is evidence that hypoxia-induced hypermethylation may be due to reduced TETs activity (55). Our findings add to this literature by suggesting that a direct interaction between hypoxia-related transcription factors and DNA methylation at specific DNA sites occur with aging, perhaps as an adaptive response triggered by fluctuations in oxygen levels that occur in many age-related conditions. This hypothesis is consistent with oxygen availability been the most important environmental factor that requires physiological adaptation during pregnancy and development and extends this concept in a life course perspective.

A limitation of this study is that we have focused on circulating cells and, therefore, our findings may not apply to age-methylation in other tissues. In addition, our findings were not replicated in an independent cross-sectional study population. In spite of these limitations, this study has unique features: a cohort of exceptionally healthy donors and

percent methylation was assessed in specific cell types obtained by cytapheresis and sorted by using state-of-the art methods.

CONCLUSION

Age-associated DNA methylation profiles of the six purified primary immune cell populations in the blood show more cell-specificity than sharedness. However, we observe common regulatory features with respect to transcription factor binding motifs and histone modifications. Based on the consistent association of these methylated sites with ARNT and REST, which are master hypoxia regulators, we hypothesize that oxygen sensing and hypoxia drive mechanisms for changes in methylation. This hypothesis should be further explored in animal models with manipulation of oxygen levels and serial measures of DNA methylation in circulating immune cells.

MATERIALS AND METHODS

Cohort details

Buffy coat, peripheral blood cells (PBMC) and granulocytes were collected from Genetic and Epigenetic Signatures of Translational Aging Laboratory Testing study (GESTALT) study participants (N=55; 34 men and 21 women; age 22-83 years) who were free of diseases (except controlled hypertension or history of cancer silent for > 10 years), not on medications (except one antihypertensive drug), had no physical or cognitive impairments, non-smokers, weighed > 110 lbs, had BMI < 30 kg/m^2 (56) (57). GESTALT was approved by the institutional review board of the National Institutes of Health and participants explicitly consented to participate.

Isolation of PBMC and immune cell populations

PBMCs were isolated from cytapheresis packs by density gradient centrifugation using Ficoll-Paque Plus. Total B, $CD4^+$ and $CD8^+$ T cells were enriched by negative selection using EasySep Negative Human kits specific for each cell type; monocytes were negatively enriched using "EasySep Human Monocyte Enrichment Kit w/o CD16 depletion". Natural killer cells were negatively enriched by depleting PBMCs with antibodies against CD3, CD4, CD14, CD19 and Glycophorin-A in HBSS buffer. Enriched cell populations were FACS sorted by flow cytometry as per Human Immunophenotyping Consortium (HIPC) phenotyping panels (58). Gating strategies and post-sort purity were analyzed by FlowJo software (LLC, Ashland, OR)(56). Granulocytes were positively selected from whole blood using EasySep™ Human Whole Blood CD66b Positive Selection Kit. Purified cells and PBMC were washed with PBS, snap frozen and stored at -80° C. All sorted cells were >95% pure by flow cytometry(56).

Assessment of DNA methylation

DNA was isolated from 1–2 million cells using DNAQuik DNA Extraction protocol and the Qiagen DNeasy Kit. 300 ng of DNA was treated with sodium bisulfite using Zymo EZ-96 DNA Methylation Kit. The methylation of ~850,000 CpG sites was determined using Illumina Human MethylationEPIC BeadChip, and data preanalyzed by GenomeStudio 2011.1.

Data processing and functional annotation of CpG sites

Analyses was performed by the R minfi package (59, 60). Probes with low detection p-values (cutoff 0.01) were filtered out(61). Data was normalized using noob and BMIQ(62), batch corrected by ComBat function (sva package), and β values were used for

differential methylation analyses. Following the MethylationEPIC probe annotation (IlluminaHumanMethylationEPICanno-.ilm10b2.hg19) to the UCSC RefSeq genes (hg19), we grouped the locations into 3 categories - 1) promoter group- TSS1500 (from 201-1500 bp upstream of TSS), TSS 200 (≤200 bp upstream of TSS), 5'UTR, first exon; 2) genebody- exons (all exons except exon1), exon intron boundary, intron and 3'UTR and 3) intergenic probes. The first gene in the annotation package was considered. Probes were divided into 3 groups-within CpG islands (CGI), within CpG shore (0-2kb from CGI), CpG shelf (2-4kb from CGI) and open sea (>4kb from CGI).

Definition of age-associated probes

Age and sex adjusted CpG-specific beta regressions were performed on normalized β values using the R *betareg* function. P-values were adjusted for multiple testing (Benjamini-Hochberg (BH) adjusted $p< 0.05$). Probes with FDR $p<0.05$ for age were considered age-differentially methylated CpGs and considered hypo- ($Estimate_{age} < 0$) or hypermethylated ($Estimate_{age} >0$). The overlap of probes across multiple combinations of the six cell types was assessed using R package SuperExactTest (v.1.1.0) (63).

Gene Set Enrichment Analysis (GSEA)

Based on the EPICarray annotation, genes were classified as differentially hypo- or hyper-methylated with age. Genes with both age hypo- and hyper-methylated CpGs were removed from the analysis. Enrichment analysis was performed by the tmodHGtest method in the tmod v.0.46.2 R package, comparing a foreground list of genes found in ≥5 cell types against reference gene set collections "Hallmarks" and "Canonical Pathways"

(which includes Reactome, KEGG, WikiPathways, PID, and Biocarta gene sets) from the Molecular Signature Database MSigDB (v.7.4)(64).

Visualization of histone peaks and DHS peaks

Primary cell DHS and chromatin ChIP-Seq bigwig files were downloaded from ENCODE (https://www.encodeproject.org/) (56). DeepTools was used to visualize DHS and histone peaks in +3kb region surrounding age-associated shared and non-shared methylated sites. For plotting purposes, the order of methylated probes was determined based on descending score of DHS peaks and followed for all histone marks (H3K4me1, H3K4me3 and H3K27ac).

Annotation of age-associated methylated probes using chromHMM

The 18-state chromHMM models (based on 6 chromatin marks H3K4me3, H3K4me1, H3K36me3, H3K27me3, H3K9me3 and H3K27ac) for various immune cells (E032- primary B cell, E038- primary naïve $CD4^+$ T cells, E047- primary naïve $CD8^+$ T cells, E029- monocyte, E046- NK cell) were downloaded from Roadmap epigenomics project (https://egg2.wustl.edu/roadmap/web_portal/chr_state_ learning.html). Bedops tool was used to map the age-associated methylated sites to the respective chromHMM profiles. All Infinium MethylationEPIC array probes were also partitioned using each of the immune cell chromHMM profiles as controls.

Prediction of de-novo transcription factor binding motifs by HOMER

±200bp around each age-associated methylated site was provided as input for analysis in HOMER using de novo setting(65).

InCHIANTI longitudinal study cohort

InCHIANTI (Invecchiare in Chianti) is a population-based cohort of individuals ≥ 20 years old from the Chianti region of Tuscany, Italy (PMID: 11129752). The Italian National Institute of Research and Care on Aging Institutional Review Board approved the study protocol and all participants explicitly consented to participate. DNA methylation from 699 participants (1841 observations) were used for the analysis. CpG methylation of 485,577 CpGs was determined by the Illumina Infinium HumanMethylation450 BeadChip (Illumina Inc., San Diego, CA) and data processed by the R package “sesame”. Mean rates of change were estimated from 2-3 longitudinal timepoints.

RNA-Seq sample extraction, processing and data analysis

Total RNA was extracted from 2 x10^6 cells, depleted from ribosomal RNA and 50ng was used for cDNA synthesis and library preparation. Libraries were sequenced for 138 cycles on Illumina HiSeq 2500. After adapter removal and end trimming of raw FASTQ files, transcript abundances were quantified with reference to hg19 transcriptome using kallisto 0.44 (with options --single -l 250 -s 25). Transcripts were aggregated to genes with tximport and filtered out if less than 10TPM were detected in more than 33% of the samples. Linear regression models (~ phase + age*sex) were used on TPM normalized expression values to study expression changes of selected transcription factors with age. female.

Data sharing statement

Microarray data are available at GEO under accession number GSE184269.

FIGURE LEGENDS

Figure 1: Study design and identification of age-associated methylation probes A) Study design. B) Age-associated CpG methylation (FDR p<0.05) in 6 cell types. C-D) SuperExactTest circular plots to show the number of age-associated hypo- and hyper-methylated probes shared among different combinations of cell types (indicated by green boxes), respectively. The outermost bars show the number of probes shared among each cell type combination (regardless of other cell types). For examples, probes hypomethylated with age in B + CD4 + CD8 + gran + mono (n=222) includes probes also hypomethylated in NK cells (n=181) and probes not hypomethylated with age in NK cells (n=41). Based on the exact probability distributions of multi-set intersections, all the overlaps shown are highly statistically significant ($p<10^{-100}$). E) Graphical representation of age-associated hypomethylation in promoter region of RCAN1 in all 6 cell types. F) Graphical representation of age-associated hypermethylation in promoter region of KLF14. The methylation status in PBMC and buffy coat are also shown. Missing methylation data is represented in white.

Figure 2: Characteristics of age-associated probes. A-B) Manhattan plot of age-associated hypo- and hypermethylated CpG sites in B cells respectively. Most significant genic probes (-log padj <10) are labelled. C) Correlation between beta-regression coefficients of age-differentially methylated CPGs in GESTALT and longitudinal InCHIANTI study. X-axis- InCHIANTI, Y-axis- B cell (Figure 2C) and $CD4^+$ T cell coefficients (Figure 2D). Blue dots - age-hypomethylated CpGs, yellow triangles- age-hypermethylated CpGs. E and F) Scatter plot of age-associated CpGs showing opposite trends in different immune cells. E) cg27123256 (in BCL11B promoter) is hypomethylated

with older age in B, monocytes and NK while is hypermethylated with older age in $CD4^+$ T cells. F) cg03530364 (in FAM19A1 promoter) is hypermethylated with older age in B, granulocytes, monocytes and NK cells while it is hypomethylated with older age in $CD4^+$ T cells.

Figure 3: Pathway analysis of methylated probes. Enrichment analysis of genes annotated to age-associated hypo- and hyper-methylated CpGs in ≥5 cell types (left-most column) and in individual cell types. Red/green shades indicate enrichment scores in hyper- (red) and hypo- (green) methylated genes. Yellow indicates ambiguous pathways associated with both hypo- and hyper-methylated genes in individual cell types. Not significant pathways are shown in grey. Full results in Supplementary Table 5.

Figure 4: Functional annotation of age-associated probes along with their grouping based on sharedness. A) ChromHMM annotation of age-associated CpGs. B) Proportion of CpGs mapping to weak/active enhancers (left, orange box), bivalent enhancers/TSS (inset, brown box) and polycomb repressor regions (right, grey box) in age-associated hypo- (blue line), hypermethylated (red line) CpGs as compared to all MethylationEPIC CpGs (grey line). C) DeepTools plots showing the distribution of accessible chromatin (DNase hypersensitive sites) and H3K4me1 histone mark in and around ± 3kb region of age-differentially methylated CpGs. The age-associated sites were divided into shared (blue) (common between 5 or more immune cells) and selective sites (green). The top row shows the pattern for age-associated hypomethylated CpGs while the bottom row is for the age-associated hypermethylated CpGs in B and $CD4^+$ T cells.

Figure 5: Association of transcription factor binding motifs with age-differentially methylated CpGs. A) Top 5 TF motifs at and around (± 200bp) of CpG sites that are hypomethylated with age. Recurring motifs like ARNT and CTCF/BORIS are highlighted. B) Top 5 TF motifs at and around (± 200bp) CpG sites that are hypermethylated with age. Recurring motifs like REST and Sp100 are highlighted. C) Hypoxia-centric model of age-associated sites with ARNT and REST motifs. CpG sites hypomethylated with aging across 6 different cell types are significantly more likely to host binding motifs for ARNT, the core hub for the hypoxia response. On the contrary, CpG sites hypermethylated with aging are significantly more likely to host binding motifs for REST, a hypoxia response transcriptional repressor. On the right are selected age-associated genes that carry the motifs for ARNT or REST transcription factors.

Acknowledgements

This work was supported entirely by the Intramural Research Program of the National Institute on Aging. We are grateful to the GESTALT participants and the GESTALT Study Team at Harbor Hospital and NIA.

Author Contributions

Conception or design of the work- N.P.W., R.S., L.F

Acquisition, analysis, or interpretation of data- R.R., P-L.K., J.C, D.S., C.U-M., D.H., M.K., S.A., A.S., A.B., J.K., A.Z.M., T.T., J.M., L.Z., C.N., T.W., C.D., R.W., W.W., Y.P., K.G.B., C.C., S.D., J.M.S.

Drafting or substantively revising the manuscript– R.R., R.S., L.F.

Conflict of interest disclosure

The authors have no conflict of interest to disclose.

REFERENCES

1. Horvath S, Raj K. DNA methylation-based biomarkers and the epigenetic clock theory of ageing. Nat Rev Genet. 2018;19(6):371-84.
2. Hannum G, Guinney J, Zhao L, Zhang L, Hughes G, Sadda S, et al. Genome-wide methylation profiles reveal quantitative views of human aging rates. Mol Cell. 2013;49(2):359-67.
3. Bocklandt S, Lin W, Sehl ME, Sanchez FJ, Sinsheimer JS, Horvath S, et al. Epigenetic predictor of age. PLoS One. 2011;6(6):e14821.
4. Gale CR, Marioni RE, Harris SE, Starr JM, Deary IJ. DNA methylation and the epigenetic clock in relation to physical frailty in older people: the Lothian Birth Cohort 1936. Clin Epigenetics. 2018;10(1):101.
5. McCartney DL, Stevenson AJ, Walker RM, Gibson J, Morris SW, Campbell A, et al. Investigating the relationship between DNA methylation age acceleration and risk factors for Alzheimer's disease. Alzheimers Dement (Amst). 2018;10:429-37.
6. Marioni RE, Shah S, McRae AF, Chen BH, Colicino E, Harris SE, et al. DNA methylation age of blood predicts all-cause mortality in later life. Genome Biol. 2015;16:25.
7. Chen BH, Marioni RE, Colicino E, Peters MJ, Ward-Caviness CK, Tsai PC, et al. DNA methylation-based measures of biological age: meta-analysis predicting time to death. Aging (Albany NY). 2016;8(9):1844-65.
8. Teschendorff AE, West J, Beck S. Age-associated epigenetic drift: implications, and a case of epigenetic thrift? Hum Mol Genet. 2013;22(R1):R7-R15.
9. Martin-Herranz DE, Aref-Eshghi E, Bonder MJ, Stubbs TM, Choufani S, Weksberg R, et al. Screening for genes that accelerate the epigenetic aging clock in humans reveals a role for the H3K36 methyltransferase NSD1. Genome Biol. 2019;20(1):146.
10. Lu AT, Xue L, Salfati EL, Chen BH, Ferrucci L, Levy D, et al. GWAS of epigenetic aging rates in blood reveals a critical role for TERT. Nat Commun. 2018;9(1):387.
11. Teschendorff AE, Menon U, Gentry-Maharaj A, Ramus SJ, Weisenberger DJ, Shen H, et al. Age-dependent DNA methylation of genes that are suppressed in stem cells is a hallmark of cancer. Genome Res. 2010;20(4):440-6.
12. Dozmorov MG, Coit P, Maksimowicz-McKinnon K, Sawalha AH. Age-associated DNA methylation changes in naive CD4(+) T cells suggest an evolving autoimmune epigenotype in aging T cells. Epigenomics. 2017;9(4):429-45.
13. Reynolds LM, Taylor JR, Ding J, Lohman K, Johnson C, Siscovick D, et al. Age-related variations in the methylome associated with gene expression in human monocytes and T cells. Nat Commun. 2014;5:5366.
14. Tserel L, Kolde R, Limbach M, Tretyakov K, Kasela S, Kisand K, et al. Age-related profiling of DNA methylation in CD8+ T cells reveals changes in immune response and transcriptional regulator genes. Sci Rep. 2015;5:13107.

15. Bell JT, Tsai PC, Yang TP, Pidsley R, Nisbet J, Glass D, et al. Epigenome-wide scans identify differentially methylated regions for age and age-related phenotypes in a healthy ageing population. PLoS Genet. 2012;8(4):e1002629.
16. Kananen L, Marttila S, Nevalainen T, Jylhava J, Mononen N, Kahonen M, et al. Aging-associated DNA methylation changes in middle-aged individuals: the Young Finns study. BMC Genomics. 2016;17:103.
17. Acevedo N, Reinius LE, Vitezic M, Fortino V, Soderhall C, Honkanen H, et al. Age-associated DNA methylation changes in immune genes, histone modifiers and chromatin remodeling factors within 5 years after birth in human blood leukocytes. Clin Epigenetics. 2015;7:34.
18. Marttila S, Kananen L, Hayrynen S, Jylhava J, Nevalainen T, Hervonen A, et al. Ageing-associated changes in the human DNA methylome: genomic locations and effects on gene expression. BMC Genomics. 2015;16:179.
19. Horvath S. DNA methylation age of human tissues and cell types. Genome Biol. 2013;14(10):R115.
20. Ferrucci L, Bandinelli S, Benvenuti E, Di Iorio A, Macchi C, Harris TB, et al. Subsystems contributing to the decline in ability to walk: bridging the gap between epidemiology and geriatric practice in the InCHIANTI study. J Am Geriatr Soc. 2000;48(12):1618-25.
21. Gray SM, Kaech SM, Staron MM. The interface between transcriptional and epigenetic control of effector and memory CD8(+) T-cell differentiation. Immunol Rev. 2014;261(1):157-68.
22. Yui MA, Rothenberg EV. Developmental gene networks: a triathlon on the course to T cell identity. Nat Rev Immunol. 2014;14(8):529-45.
23. de Oliveira PG, Ramos MLS, Amaro AJ, Dias RA, Vieira SI. Gi/o-Protein Coupled Receptors in the Aging Brain. Front Aging Neurosci. 2019;11:89.
24. Ernst J, Kellis M. ChromHMM: automating chromatin-state discovery and characterization. Nat Methods. 2012;9(3):215-6.
25. Pundhir S, Bagger FO, Lauridsen FB, Rapin N, Porse BT. Peak-valley-peak pattern of histone modifications delineates active regulatory elements and their directionality. Nucleic Acids Res. 2016;44(9):4037-51.
26. Bae S, Lesch BJ. H3K4me1 Distribution Predicts Transcription State and Poising at Promoters. Front Cell Dev Biol. 2020;8:289.
27. Medvedeva YA, Khamis AM, Kulakovskiy IV, Ba-Alawi W, Bhuyan MS, Kawaji H, et al. Effects of cytosine methylation on transcription factor binding sites. BMC Genomics. 2014;15:119.
28. Moore LD, Le T, Fan G. DNA methylation and its basic function. Neuropsychopharmacology. 2013;38(1):23-38.
29. Kim C, Jin J, Weyand CM, Goronzy JJ. The Transcription Factor TCF1 in T Cell Differentiation and Aging. Int J Mol Sci. 2020;21(18).
30. van Ruiten MS, Rowland BD. On the choreography of genome folding: A grand pas de deux of cohesin and CTCF. Curr Opin Cell Biol. 2021;70:84-90.
31. Bhat P, Honson D, Guttman M. Nuclear compartmentalization as a mechanism of quantitative control of gene expression. Nat Rev Mol Cell Biol. 2021;22(10):653-70.
32. Yuan T, Jiao Y, de Jong S, Ophoff RA, Beck S, Teschendorff AE. An integrative multi-scale analysis of the dynamic DNA methylation landscape in aging. PLoS Genet. 2015;11(2):e1004996.
33. Lu T, Aron L, Zullo J, Pan Y, Kim H, Chen Y, et al. REST and stress resistance in ageing and Alzheimer's disease. Nature. 2014;507(7493):448-54.
34. Nyati KK, Zaman MM, Sharma P, Kishimoto T. Arid5a, an RNA-Binding Protein in Immune Regulation: RNA Stability, Inflammation, and Autoimmunity. Trends Immunol. 2020;41(3):255-68.
35. Wilsker D, Patsialou A, Dallas PB, Moran E. ARID proteins: a diverse family of DNA binding proteins implicated in the control of cell growth, differentiation, and development. Cell Growth Differ. 2002;13(3):95-106.

36. Semenza GL. HIF-1: mediator of physiological and pathophysiological responses to hypoxia. J Appl Physiol (1985). 2000;88(4):1474-80.
37. Craps S, Van Wauwe J, De Moudt S, De Munck D, Leloup AJA, Boeckx B, et al. Prdm16 Supports Arterial Flow Recovery by Maintaining Endothelial Function. Circ Res. 2021;129(1):63-77.
38. Stegmann TJ. FGF-1: a human growth factor in the induction of neoangiogenesis. Expert Opin Investig Drugs. 1998;7(12):2011-5.
39. Chakraborty S, Ain R. Nitric-oxide synthase trafficking inducer is a pleiotropic regulator of endothelial cell function and signaling. J Biol Chem. 2017;292(16):6600-20.
40. Gusdon AM, Zhu J, Van Houten B, Chu CT. ATP13A2 regulates mitochondrial bioenergetics through macroautophagy. Neurobiol Dis. 2012;45(3):962-72.
41. Wang J, Taba Y, Pang J, Yin G, Yan C, Berk BC. GIT1 mediates VEGF-induced podosome formation in endothelial cells: critical role for PLCgamma. Arterioscler Thromb Vasc Biol. 2009;29(2):202-8.
42. Hsu C, Morohashi Y, Yoshimura S, Manrique-Hoyos N, Jung S, Lauterbach MA, et al. Regulation of exosome secretion by Rab35 and its GTPase-activating proteins TBC1D10A-C. J Cell Biol. 2010;189(2):223-32.
43. Pamenter ME, Hall JE, Tanabe Y, Simonson TS. Cross-Species Insights Into Genomic Adaptations to Hypoxia. Front Genet. 2020;11:743.
44. Pangou E, Befani C, Mylonis I, Samiotaki M, Panayotou G, Simos G, et al. HIF-2alpha phosphorylation by CK1delta promotes erythropoietin secretion in liver cancer cells under hypoxia. J Cell Sci. 2016;129(22):4213-26.
45. Lazarou M, Narendra DP, Jin SM, Tekle E, Banerjee S, Youle RJ. PINK1 drives Parkin self-association and HECT-like E3 activity upstream of mitochondrial binding. J Cell Biol. 2013;200(2):163-72.
46. Cai ZL, Liu C, Yao Q, Xie QW, Hu TT, Wu QQ, et al. The pro-migration and anti-apoptosis effects of HMGA2 in HUVECs stimulated by hypoxia. Cell Cycle. 2020;19(24):3534-45.
47. Tan WS, Lee JJ, Satish RL, Ang ET. Detectability of secretagogin in human erythrocytes. Neurosci Lett. 2012;526(1):59-62.
48. Liu TJ, Yeh YC, Lee WL, Wang LC, Lee HW, Shiu MT, et al. Insulin ameliorates hypoxia-induced autophagy, endoplasmic reticular stress and apoptosis of myocardial cells: In vitro and ex vivo models. Eur J Pharmacol. 2020;880:173125.
49. Dasgupta P. Somatostatin analogues: multiple roles in cellular proliferation, neoplasia, and angiogenesis. Pharmacol Ther. 2004;102(1):61-85.
50. Carmeliet P, Jain RK. Molecular mechanisms and clinical applications of angiogenesis. Nature. 2011;473(7347):298-307.
51. Cavadas MA, Mesnieres M, Crifo B, Manresa MC, Selfridge AC, Keogh CE, et al. REST is a hypoxia-responsive transcriptional repressor. Sci Rep. 2016;6:31355.
52. Gu Y, Luo M, Li Y, Su Z, Wang Y, Chen X, et al. Bcl6 knockdown aggravates hypoxia injury in cardiomyocytes via the P38 pathway. Cell Biol Int. 2019;43(2):108-16.
53. Matsuyama M, WuWong DJ, Horvath S, Matsuyama S. Epigenetic clock analysis of human fibroblasts in vitro: effects of hypoxia, donor age, and expression of hTERT and SV40 largeT. Aging (Albany NY). 2019;11(10):3012-22.
54. Shahrzad S, Bertrand K, Minhas K, Coomber BL. Induction of DNA hypomethylation by tumor hypoxia. Epigenetics. 2007;2(2):119-25.
55. Thienpont B, Steinbacher J, Zhao H, D'Anna F, Kuchnio A, Ploumakis A, et al. Tumour hypoxia causes DNA hypermethylation by reducing TET activity. Nature. 2016;537(7618):63-8.
56. Roy R, Ramamoorthy S, Shapiro BD, Kaileh M, Hernandez D, Sarantopoulou D, et al. DNA methylation signatures reveal that distinct combinations of transcription factors specify human immune cell epigenetic identity. Immunity. 2021.

57. Ubaida-Mohien C, Gonzalez-Freire M, Lyashkov A, Moaddel R, Chia CW, Simonsick EM, et al. Physical Activity Associated Proteomics of Skeletal Muscle: Being Physically Active in Daily Life May Protect Skeletal Muscle From Aging. Front Physiol. 2019;10:312.
58. Maecker HT, McCoy JP, Nussenblatt R. Standardizing immunophenotyping for the Human Immunology Project. Nat Rev Immunol. 2012;12(3):191-200.
59. Aryee MJ, Jaffe AE, Corrada-Bravo H, Ladd-Acosta C, Feinberg AP, Hansen KD, et al. Minfi: a flexible and comprehensive Bioconductor package for the analysis of Infinium DNA methylation microarrays. Bioinformatics. 2014;30(10):1363-9.
60. Fortin JP, Triche TJ, Jr., Hansen KD. Preprocessing, normalization and integration of the Illumina HumanMethylationEPIC array with minfi. Bioinformatics. 2017;33(4):558-60.
61. Moran S, Arribas C, Esteller M. Validation of a DNA methylation microarray for 850,000 CpG sites of the human genome enriched in enhancer sequences. Epigenomics. 2016;8(3):389-99.
62. Liu J, Siegmund KD. An evaluation of processing methods for HumanMethylation450 BeadChip data. BMC Genomics. 2016;17:469.
63. Wang M, Zhao Y, Zhang B. Efficient Test and Visualization of Multi-Set Intersections. Sci Rep. 2015;5:16923.
64. Subramanian A, Tamayo P, Mootha VK, Mukherjee S, Ebert BL, Gillette MA, et al. Gene set enrichment analysis: a knowledge-based approach for interpreting genome-wide expression profiles. Proc Natl Acad Sci U S A. 2005;102(43):15545-50.
65. Heinz S, Benner C, Spann N, Bertolino E, Lin YC, Laslo P, et al. Simple combinations of lineage-determining transcription factors prime cis-regulatory elements required for macrophage and B cell identities. Mol Cell. 2010;38(4):576-89.

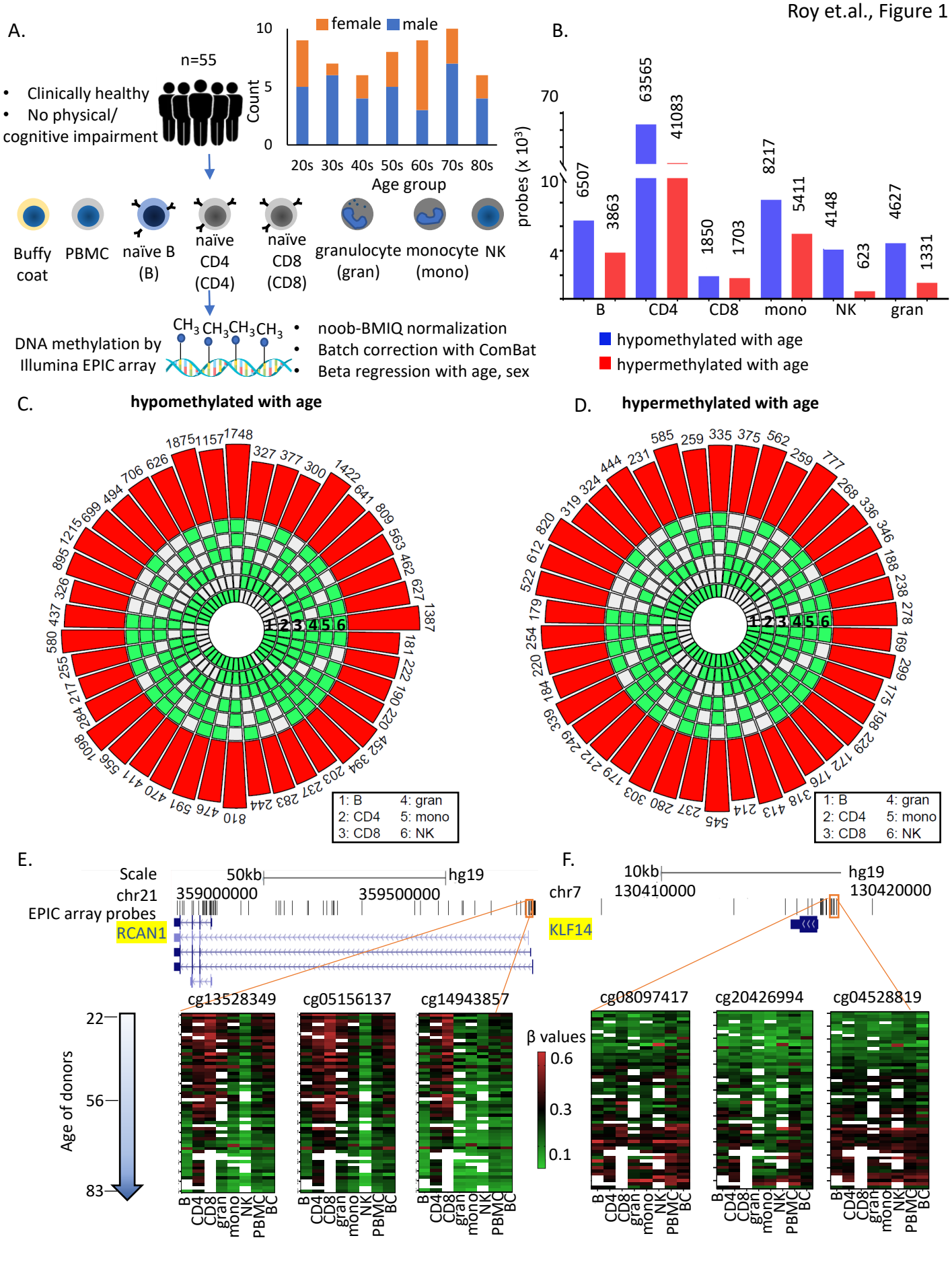
A.
n=55
Clinically healthy
No physical/ cognitive impairment
female
male
Count
Age group
20s 30s 40s 50s 60s 70s 80s
Buffy coat
PBMC
naïve B (B)
naïve CD4 (CD4)
naïve CD8 (CD8)
granulocyte (gran)
monocyte (mono)
NK
DNA methylation by Illumina EPIC array
noob-BMIQ normalization
Batch correction with ComBat
Beta regression with age, sex
B.
probes (x 10³)
6507
3863
63565
41083
1850
1703
8217
5411
4148
623
4627
1331
B
CD4
CD8
mono
NK
gran
hypomethylated with age
hypermethylated with age
C.
hypomethylated with age
D.
hypermethylated with age
1: B
2: CD4
3: CD8
4: gran
5: mono
6: NK
E.
Scale
50kb
hg19
chr21
359000000
359500000
EPIC array probes
RCAN1
cg13528349
cg05156137
cg14943857
Age of donors
22
56
83
β values
0.6
0.3
0.1
F.
10kb
hg19
chr7
130410000
130420000
KLF14
cg08097417
cg20426994
cg04528819

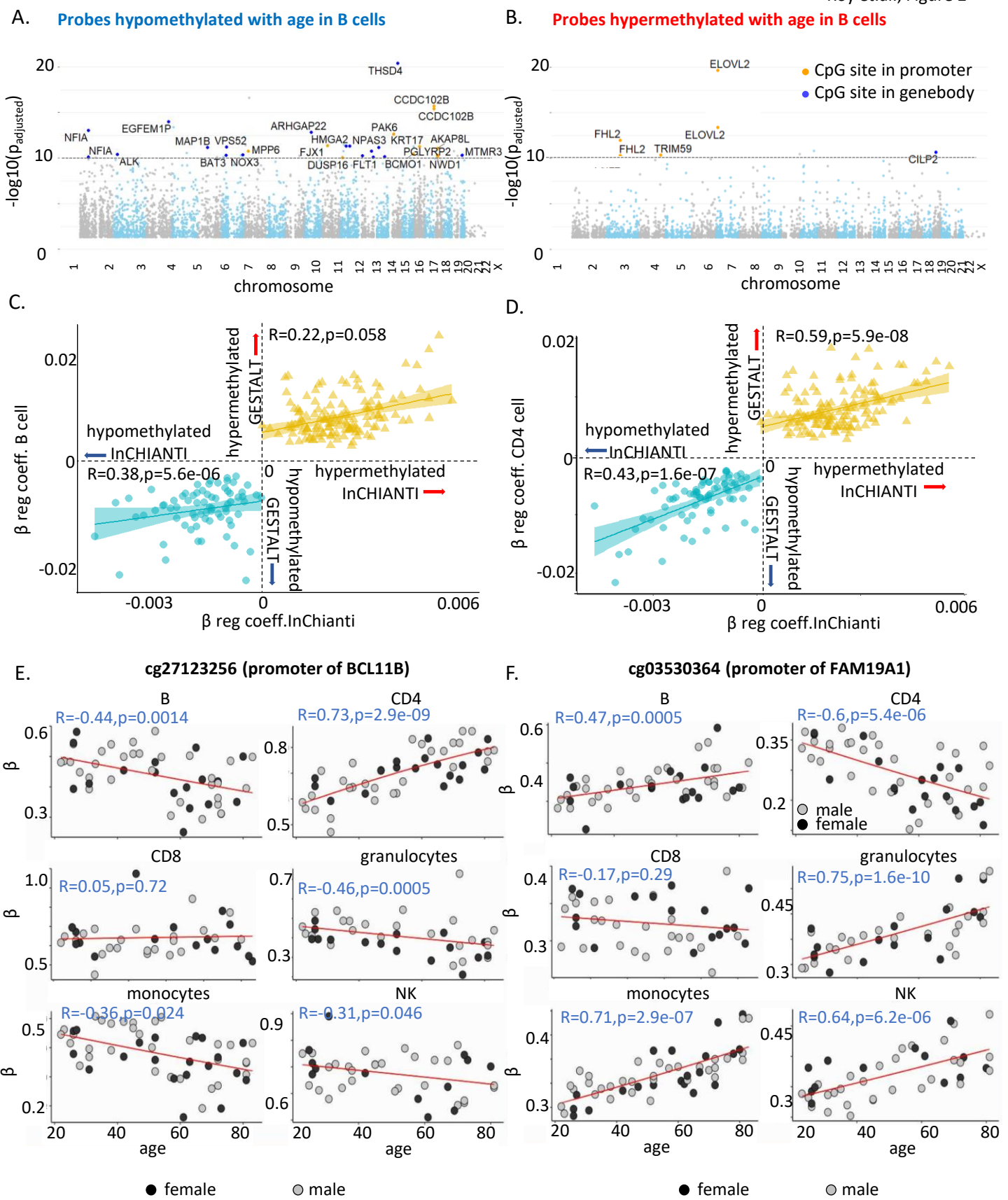
A.
Probes hypomethylated with age in B cells
B.
Probes hypermethylated with age in B cells
-log10(p adjusted)
chromosome
THSD4
CCDC102B
CCDC102B
EGFEM1P
ARHGAP22
PAK6
NFIA
MAP1B
VPS52
HMGA2
NPAS3
KRT17
AKAP8L
NFIA
MPP6
FJX1
PGLYRP2
MTMR3
ALK
BAT3
NOX3
DUSP16
FLT1
BCMO1
NWD1
ELOVL2
CpG site in promoter
CpG site in genebody
FHL2
ELOVL2
FHL2
TRIM59
CILP2
C.
D.
β reg coeff. B cell
β reg coeff. CD4 cell
β reg coeff.InChianti
hypomethylated
InCHIANTI
hypermethylated
GESTALT
R=0.22,p=0.058
R=0.38,p=5.6e-06
R=0.59,p=5.9e-08
R=0.43,p=1.6e-07
E.
cg27123256 (promoter of BCL11B)
F.
cg03530364 (promoter of FAM19A1)
B
CD4
CD8
granulocytes
monocytes
NK
R=-0.44,p=0.0014
R=0.73,p=2.9e-09
R=0.05,p=0.72
R=-0.46,p=0.0005
R=-0.36,p=0.024
R=-0.31,p=0.046
R=0.47,p=0.0005
R=-0.6,p=5.4e-06
R=-0.17,p=0.29
R=0.75,p=1.6e-10
R=0.71,p=2.9e-07
R=0.64,p=6.2e-06
β
age
male
female

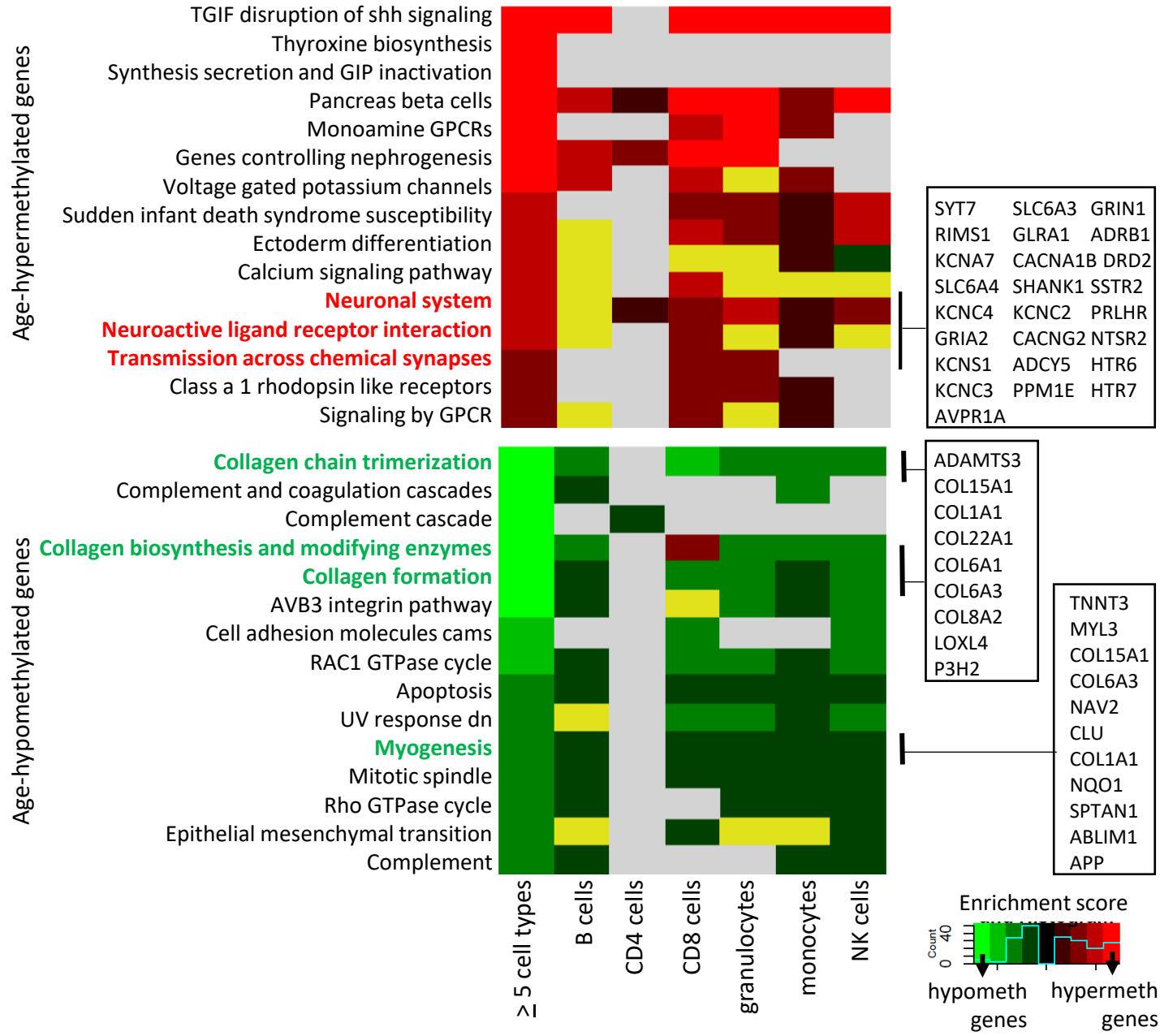
Age-hypermethylated genes
TGIF disruption of shh signaling
Thyroxine biosynthesis
Synthesis secretion and GIP inactivation
Pancreas beta cells
Monoamine GPCRs
Genes controlling nephrogenesis
Voltage gated potassium channels
Sudden infant death syndrome susceptibility
Ectoderm differentiation
Calcium signaling pathway
Neuronal system
Neuroactive ligand receptor interaction
Transmission across chemical synapses
Class a 1 rhodopsin like receptors
Signaling by GPCR
SYT7 SLC6A3 GRIN1
RIMS1 GLRA1 ADRB1
KCNA7 CACNA1B DRD2
SLC6A4 SHANK1 SSTR2
KCNC4 KCNC2 PRLHR
GRIA2 CACNG2 NTSR2
KCNS1 ADCY5 HTR6
KCNC3 PPM1E HTR7
AVPR1A
Age-hypomethylated genes
Collagen chain trimerization
Complement and coagulation cascades
Complement cascade
Collagen biosynthesis and modifying enzymes
Collagen formation
AVB3 integrin pathway
Cell adhesion molecules cams
RAC1 GTPase cycle
Apoptosis
UV response dn
Myogenesis
Mitotic spindle
Rho GTPase cycle
Epithelial mesenchymal transition
Complement
ADAMTS3
COL15A1
COL1A1
COL22A1
COL6A1
COL6A3
COL8A2
LOXL4
P3H2
TNNT3
MYL3
COL15A1
COL6A3
NAV2
CLU
COL1A1
NQO1
SPTAN1
ABLIM1
APP
≥ 5 cell types
B cells
CD4 cells
CD8 cells
granulocytes
monocytes
NK cells
Enrichment score
Count
0 40
hypometh genes
hypermeth genes
N.S(q>0.05)
mixed(showing both hypo and hypermethylation with age)

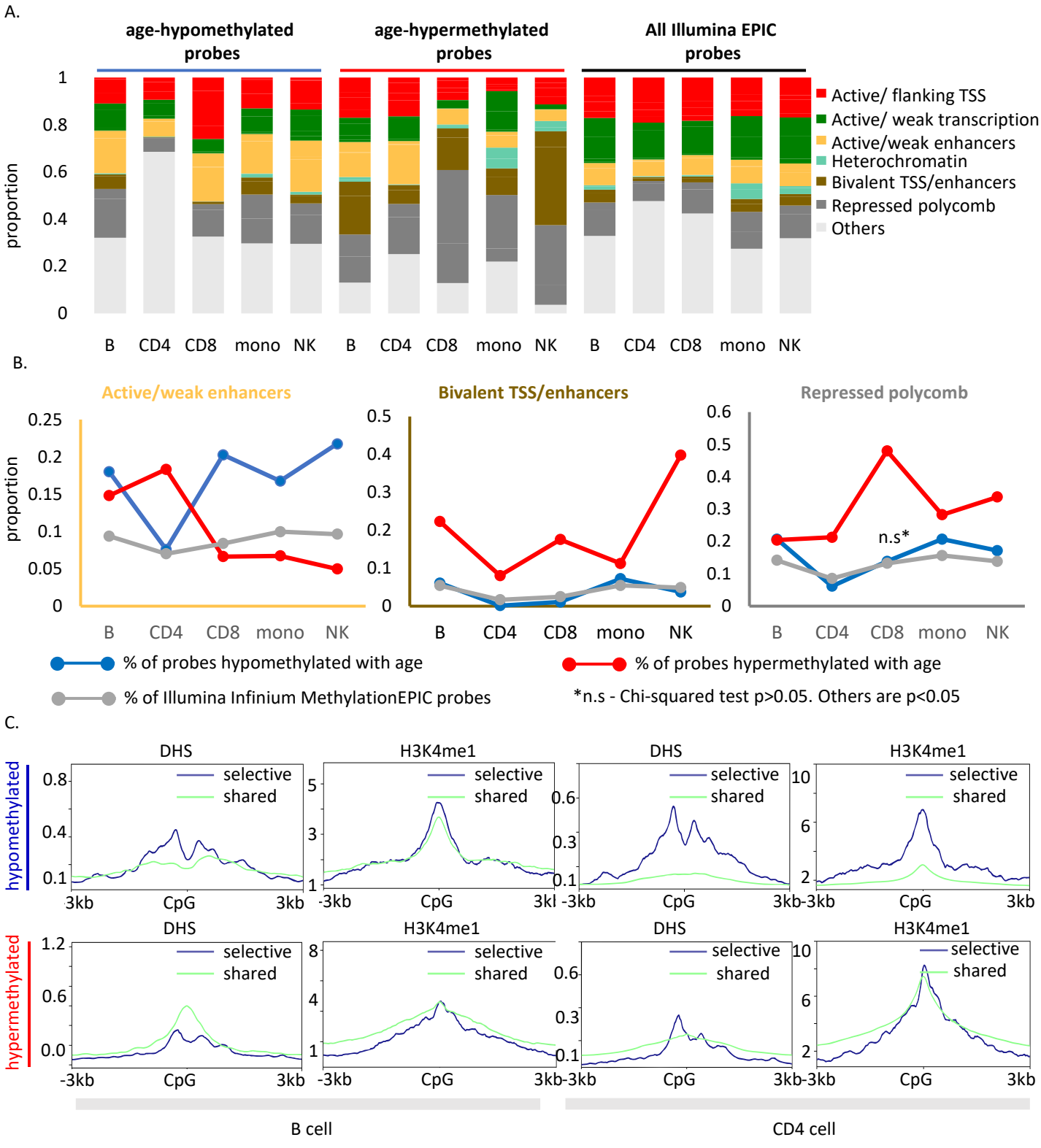
A.
age-hypomethylated probes
age-hypermethylated probes
All Illumina EPIC probes
proportion
Active/ flanking TSS
Active/ weak transcription
Active/weak enhancers
Heterochromatin
Bivalent TSS/enhancers
Repressed polycomb
Others
B CD4 CD8 mono NK
B.
Active/weak enhancers
Bivalent TSS/enhancers
Repressed polycomb
n.s*
% of probes hypomethylated with age
% of probes hypermethylated with age
% of Illumina Infinium MethylationEPIC probes
*n.s - Chi-squared test p>0.05. Others are p<0.05
C.
hypomethylated
hypermethylated
DHS
H3K4me1
selective
shared
3kb CpG 3kb
-3kb CpG 3kb
B cell
CD4 cell

A. Hypomethylated with age

B. Hypermethylated with age

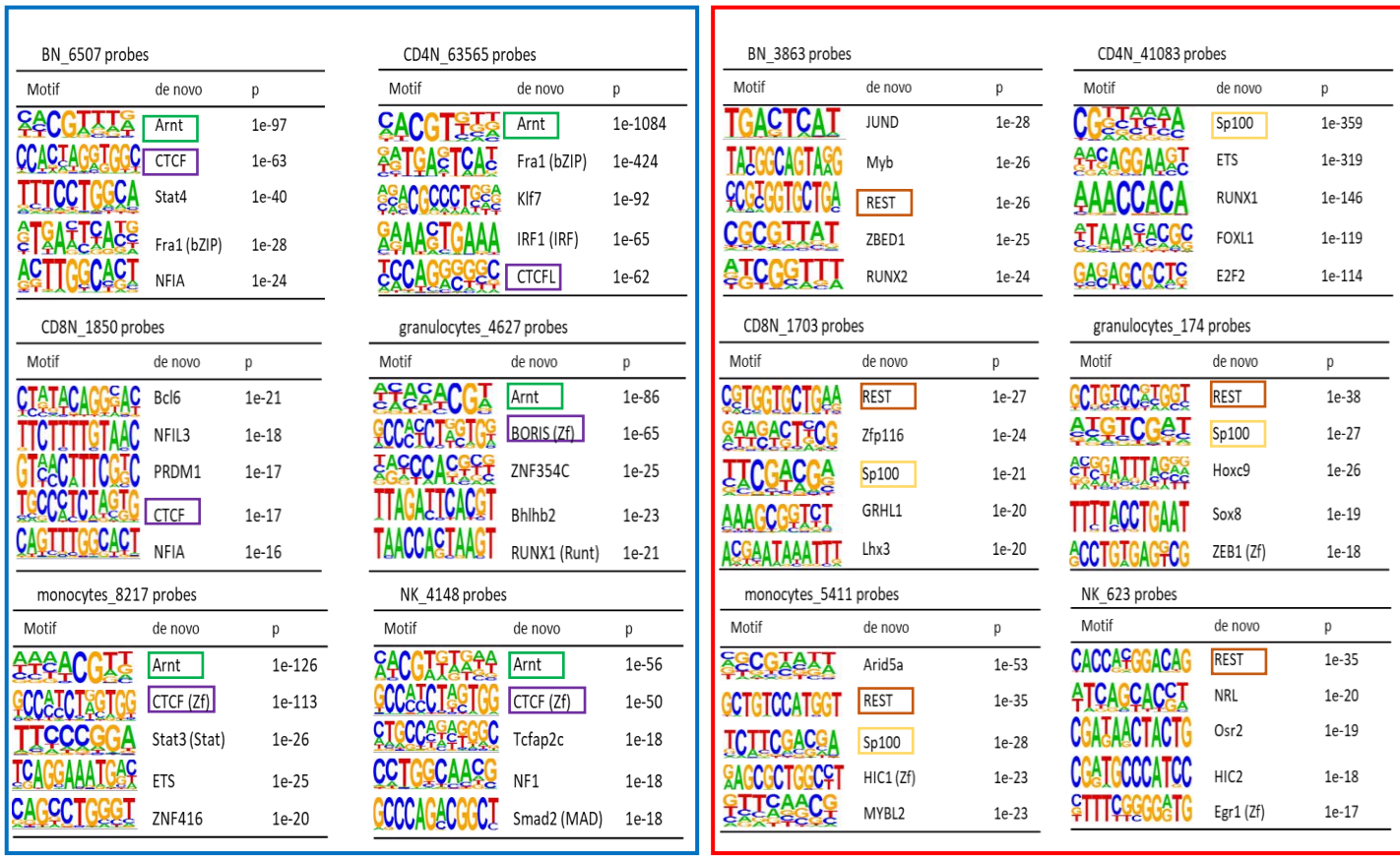

C.

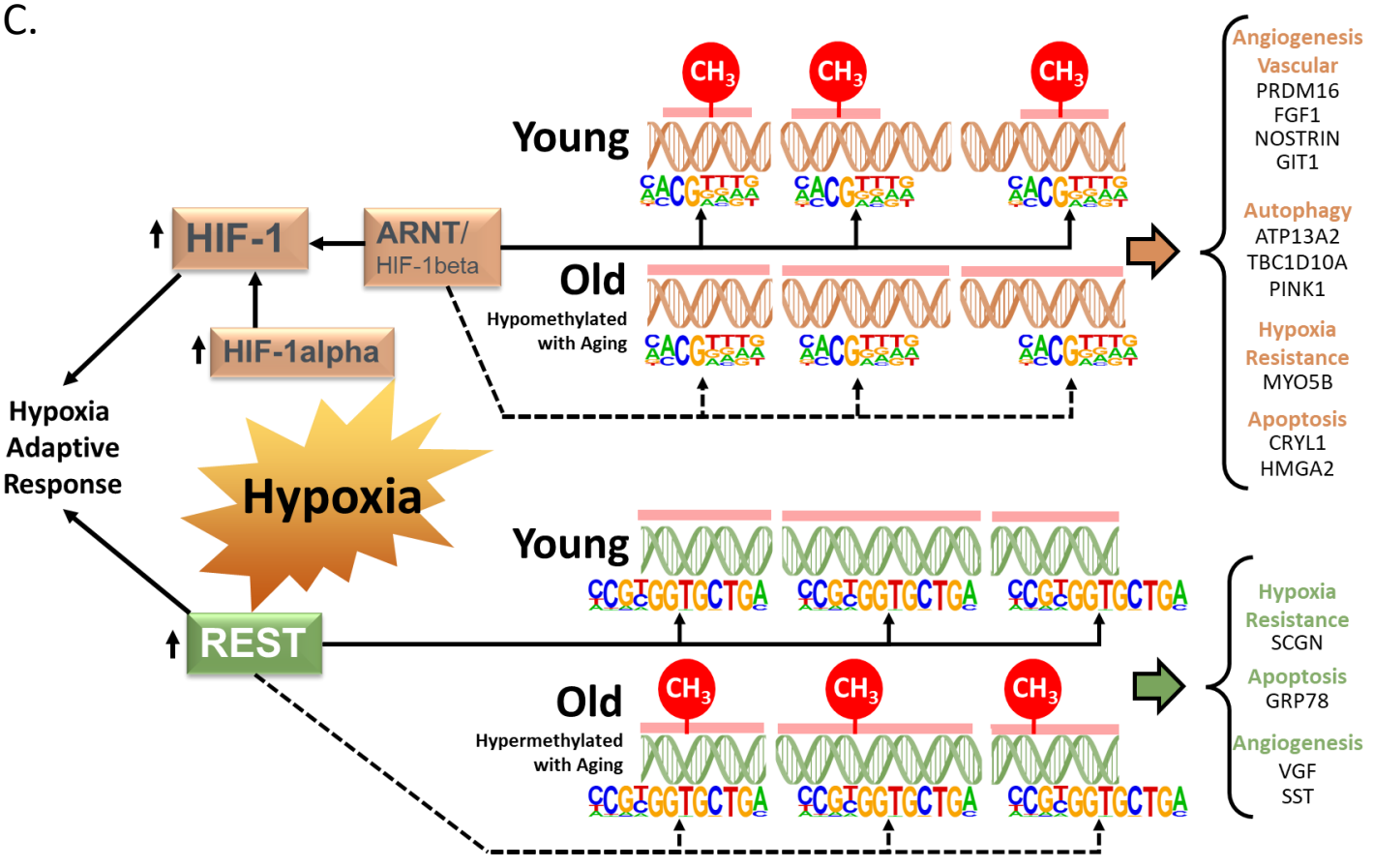

SUPPLEMENTARY FIGURE LEGENDS

Supplementary Figure 1: Characteristics of entire dataset and age-associated methylation data in 6 primary immune cells. A) PCA plot of normalized methylation data of six immune cells in the 55 healthy donors. The cell types are indicated in different colors, while the three broad age groups (20-40, 40-60 and 60-90 years) are indicated in different shapes (PC1- principal component 1, PC2- principal component 2). B) Distribution of beta-regression coefficient of the age-associated hypo- and hypermethylated probes in all six immune cell types estimated this cross-sectional study. Distribution of coefficient values categorized into groups is shown in Supplementary Table 2. C). Age-associated probes from independent sample t-test analysis of young (<=35years, 25th percentile) vs old (>=70years, 75th percentile) donors for each cell type. The pie charts on top show the extent of overlap with results from the beta-regression analysis. D) Distribution of age-associated probes from beta regression into groups based on distance from CpG islands (CGI) (Island- within CGI, shore- within 2kb of CGI, shelf- 2-4kb of CGI, open sea- >4kb from CGI). E) Distribution of age-associated hypo- and hypermethylated probes with respect to location (promoter-1500TSS to 1st exon, genebody-within exons, introns and 3'UTR). F and G) Overlap of age-associated hypo- and hypermethylated probes in the 6 immune cell types with those identified in PBMCs. The first bar indicates the number of age-associated probes identified in PBMC. The following bars show the counts in the other immune cells, the lighter portion of the bars show the number of probes that are shared with PBMCs, and the darker portion indicates non-PBMC cell-specific probes. The tables below show the log of odd's ratio and its 95%

confidence interval to represent of the significance of the overlap between age-associated probes in each cell type with PBMC.

Supplementary Figure 2: Most significant age-associated CpGs in non-B immune cells along with CpGs showing opposite age-associated trends. A) Manhattan plot of age-associated CpGs in $CD4^+$ T cells. The X-axis shows the distribution of significant CpGs (FDR $p<0.05$), and the Y-axis shows the associated negative log of the adjusted p value from beta regression. Positive axis comprises of probes hypermethylated with age while the negative axis shows age-associated hypomethylated probes. The top hits in each group with the most significant p-values are labelled where the orange dot present CpG probes in the gene promoter. B) Manhattan plot of age-associated probes in $CD8^+$ T cells. C) Manhattan plot of age-associated probes in granulocytes. D) Manhattan plot of age-associated probes in NK cells. E) Manhattan plot of age-associated probes in monocytes. F) Count of probes hypomethylated with age in cell type of interest but showing hypermethylation in one or more other cell types. For example, 315 probes are age-hypomethylated in B cells but are significantly hypermethylated with age in one or more other immune cell types. Maximum number of such probes are observed in $CD4^+$ T cells followed by B cells and monocytes. G) Count of probes hypermethylated with age in cell type of interest but showing hypomethylation in one or more other cell types. For example, 282 probes are hypermethylated in B cells but are significantly hypomethylated with age in one or more other immune cell types. Maximum number of such probes are observed in $CD4^+$ T cells followed by B cells and monocytes.

Supplementary Figure 3: Comparison individual immune cells with InCHIANTI longitudinal study. A-B) Correlation between beta-regression coefficients of age-

associated methylation probes in 5 or more cell types in study and beta-regression coefficients estimated from longitudinal data in the InCHIANTI study. On the X-axis is the data from InCHIANTI longitudinal study cohort while on the Y-axis is cell-specific coefficient values for $CD8^+$ T cells (top left), granulocytes (top right), monocytes (bottom left) and NK cells (bottom right). pink dots are the coefficients of the age-hypomethylated probes (Supplementary Figure 3A) while the blue dots are for age-hypermethylated probes (Supplementary Figure 3B).

Supplementary Figure 4: Functional annotation of age-associated probes with respect to DHS and histone marks from ENCODE. The functional significance of age-associated probes with respect to other epigenetic marks was examined using the DNase hypersensitivity sites and H3K4me1 peaks on primary immune cells from ENCODE. Granulocyte data was not available and hence could not be examined. Age-associated hypo- or hypermethylated probes were grouped into shared (blue) and selective (green) based on whether they were common across 5 or more of the 6 cell types. A region of 3kb of either side of the CpG probes of interest was examined.

Supplementary Figure 5: Count of age-associated hypo- or hypermethylated probes with ARNT or REST motifs within 1kb respectively. ARNT and REST were the top TF motifs associated respectively with all hypo- and hypermethylated age-associated probes in most cell types. To verify whether the same set of probes were present in each cell type with the ARNT(A) or REST(B) motifs, HOMER was used to find the probes that have a ARNT or REST motif within $\pm$ 500bp. The SuperExact test based circular plots shows the overlap between the different cell types (relevant cell types are indicated in green boxes in the inner circles for each combination). The numbers above

the outermost bars indicate the count of probes that have ARNT or REST motifs across various combinations of cells while the color of the outermost bars in the plot indicate the log transformed p values obtained from hypergeometric test to check whether the overlap is significant or not.

LIST OF SUPPLMENTARY TABLES

Supplementary Table 1: Demographic and flow cytometry marker details of the cohort. Details of the age and sex distribution of the healthy donors from the GESTALT study for each of the primary immune cell type population are described. The flow cytometry markers for cell selection are also mentioned.

Supplementary Table 2: Distribution of slope for probes significantly changing with age in the immune cells. The age-associated probes were identified from beta regression (FDR $p<0.05$).

Supplementary Table 3: List of most significant age-associated probes in the immune cells. Based on a p-value cut off (-log (FDR adjusted p) >10), the top age-associated candidates were studied to search for common genes across all immune cells.

Supplementary Table 4: List of top age-associated genes in the six immune cell types. The list of genes from top 50 age-associated hypo- and hypermethylated probes.

Supplementary Table 5: Detailed output of Gene Set Enrichment Analysis. Gene Set Enrichment Analysis was performed on genes based on annotation of age-associated hypo- and hypermethylation probes commonly changing in 5 or more cell types.

Supplementary Table 6: Age-associated differences of transcripts for ARNT, REST and CTCF. RNASeq data was used to look into the gene expression change of the selected transcription factors with age. These transcription factor motifs are most commonly associated with the age-related methylated sites in all immune cells.

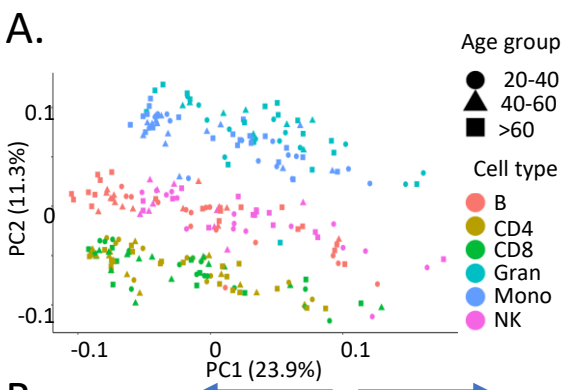

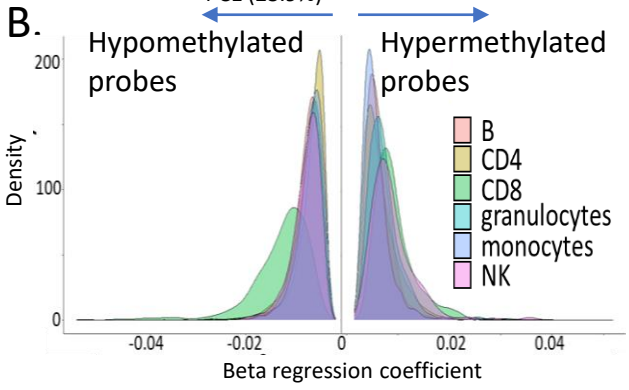

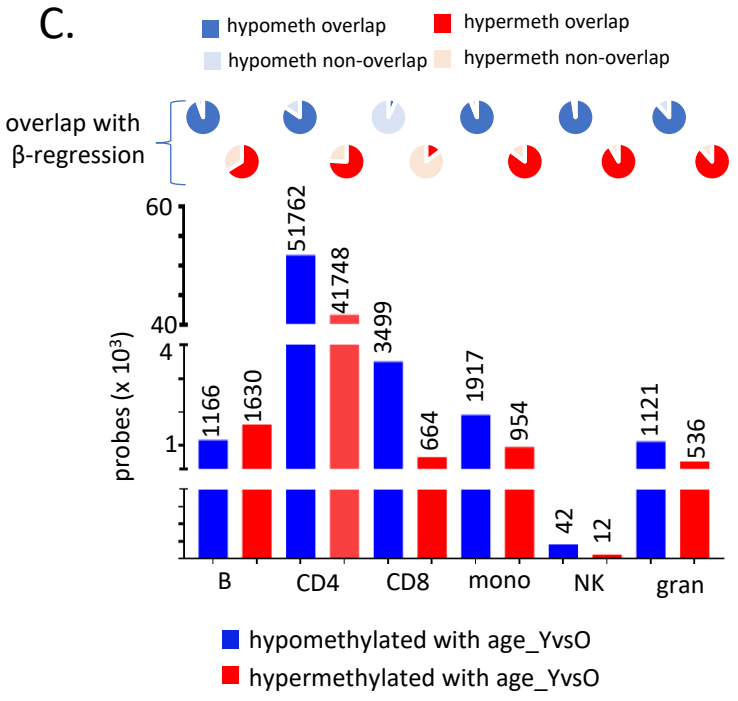

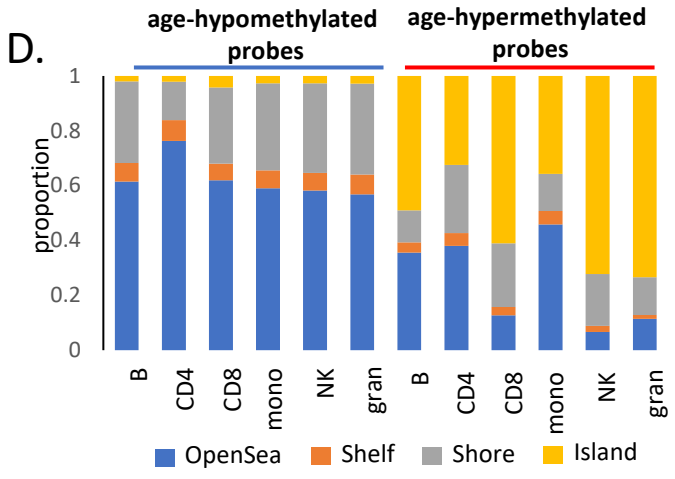

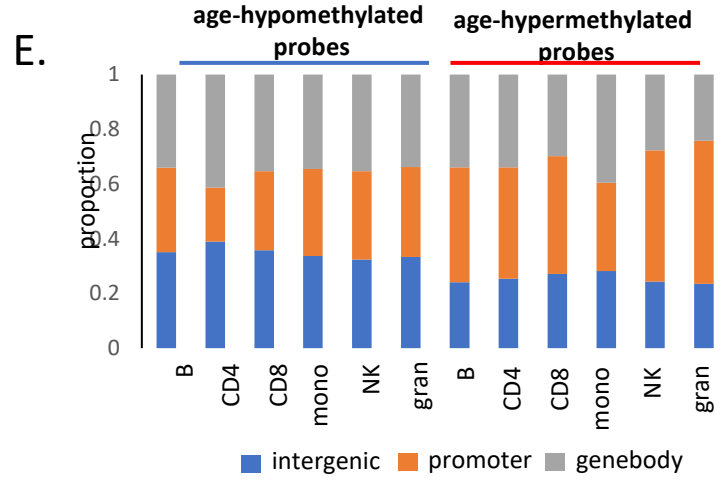

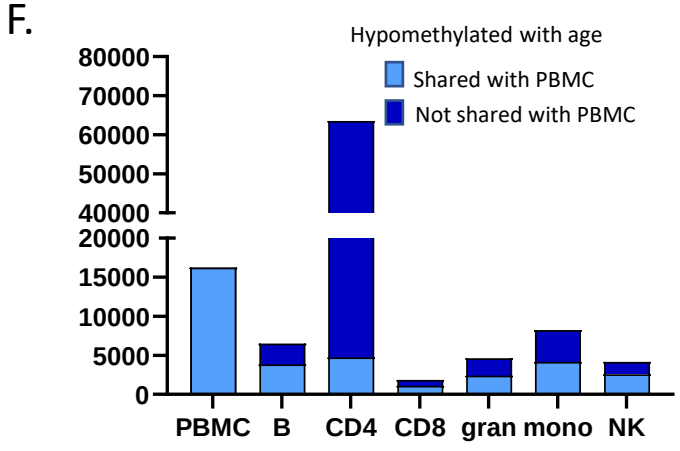

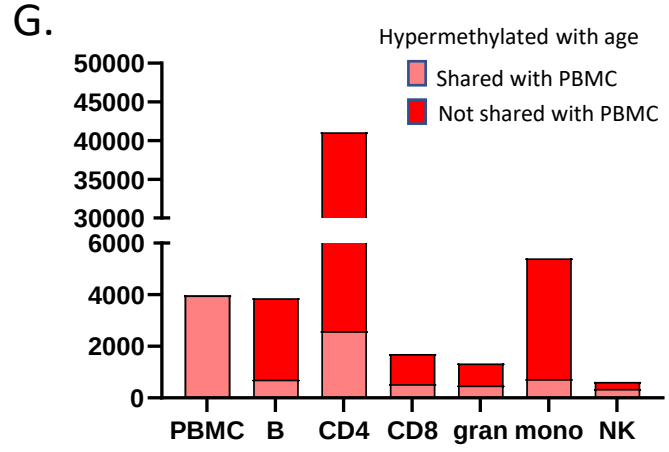

	B	CD4	CD8	gran	mono	NK
log Odd's ratio	1.99	0.74	1.92	1.82	1.86	2.00
95% C.I_lower	1.97	0.73	1.87	1.79	1.83	1.98
95% C.I_upper	2.02	0.76	1.96	1.85	1.88	2.03
p value	<0.01	<0.01	<0.01	<0.01	<0.01	<0.01

	B	CD4	CD8	gran	mono	NK
log Odd's ratio	1.77	1.60	2.07	2.14	1.62	2.49
95% C.I_lower	1.73	1.58	2.02	2.09	1.58	2.41
95% C.I_upper	1.81	1.63	2.11	2.19	1.65	2.56
p value	<0.01	<0.01	<0.01	<0.01	<0.01	<0.01

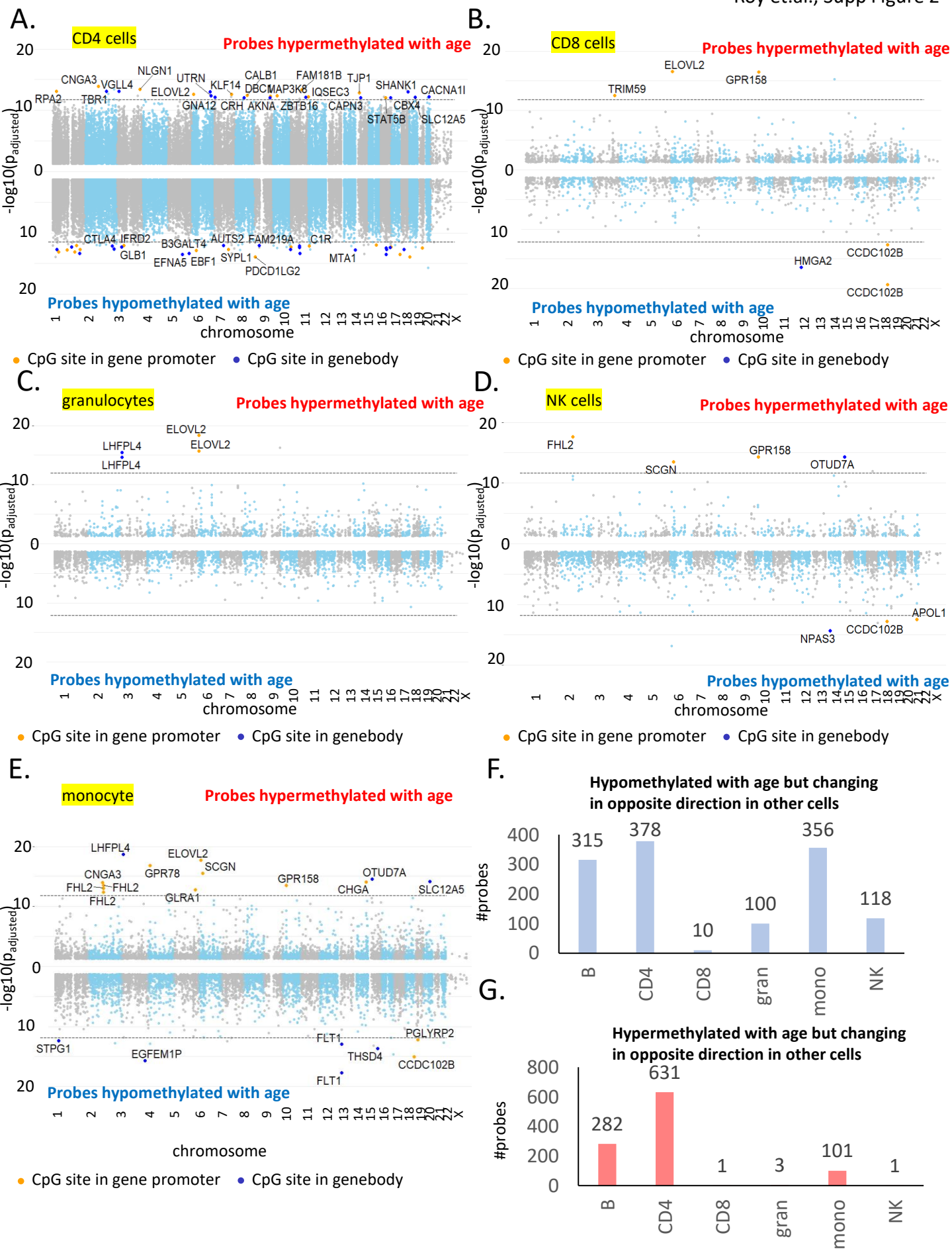
A.
CD4 cells
Probes hypermethylated with age
Probes hypomethylated with age
-log10(padjusted)
chromosome
CpG site in gene promoter
CpG site in genebody
B.
CD8 cells
Probes hypermethylated with age
Probes hypomethylated with age
-log10(padjusted)
chromosome
CpG site in gene promoter
CpG site in genebody
C.
granulocytes
Probes hypermethylated with age
Probes hypomethylated with age
-log10(padjusted)
chromosome
CpG site in gene promoter
CpG site in genebody
D.
NK cells
Probes hypermethylated with age
Probes hypomethylated with age
-log10(padjusted)
chromosome
CpG site in gene promoter
CpG site in genebody
E.
monocyte
Probes hypermethylated with age
Probes hypomethylated with age
-log10(padjusted)
chromosome
CpG site in gene promoter
CpG site in genebody
F.
Hypomethylated with age but changing in opposite direction in other cells
#probes
315
378
10
100
356
118
B
CD4
CD8
gran
mono
NK
G.
Hypermethylated with age but changing in opposite direction in other cells
#probes
282
631
1
3
101
1
B
CD4
CD8
gran
mono
NK

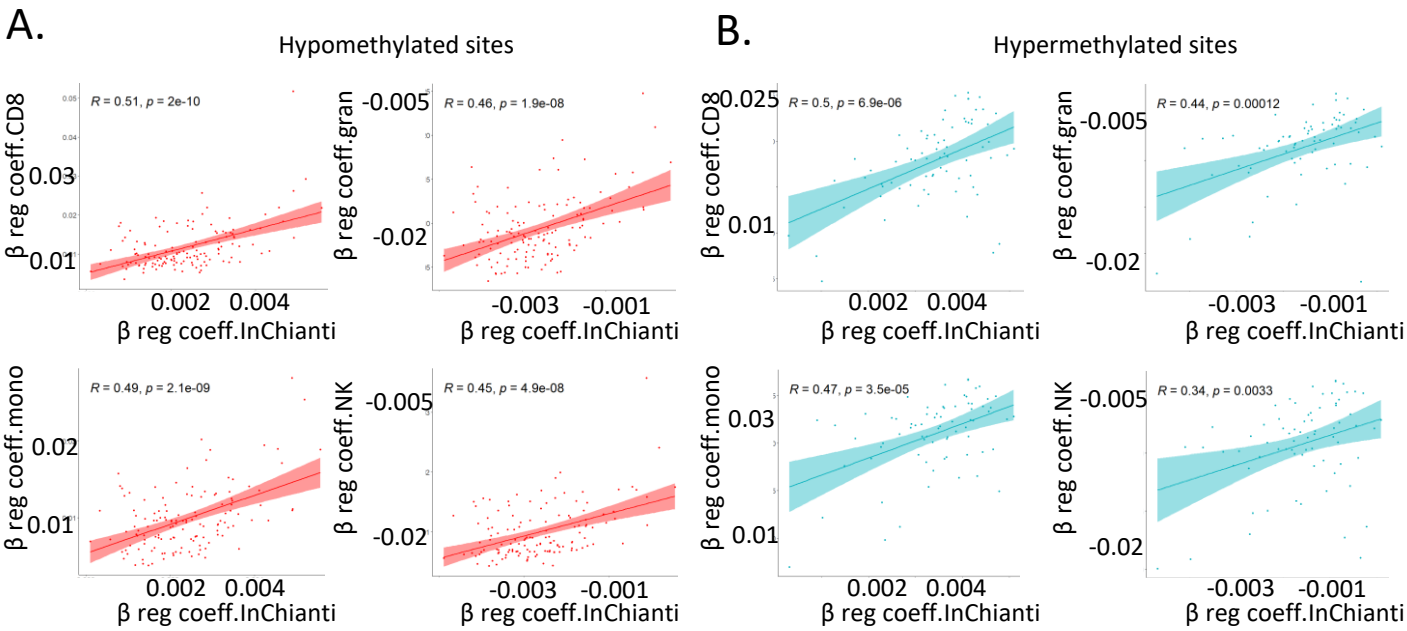
A.
Hypomethylated sites
B.
Hypermethylated sites
R = 0.51, p = 2e-10
β reg coeff.CD8
β reg coeff.InChianti
R = 0.46, p = 1.9e-08
β reg coeff.gran
β reg coeff.InChianti
R = 0.5, p = 6.9e-06
β reg coeff.CD8
β reg coeff.InChianti
R = 0.44, p = 0.00012
β reg coeff.gran
β reg coeff.InChianti
R = 0.49, p = 2.1e-09
β reg coeff.mono
β reg coeff.InChianti
R = 0.45, p = 4.9e-08
β reg coeff.NK
β reg coeff.InChianti
R = 0.47, p = 3.5e-05
β reg coeff.mono
β reg coeff.InChianti
R = 0.34, p = 0.0033
β reg coeff.NK
β reg coeff.InChianti

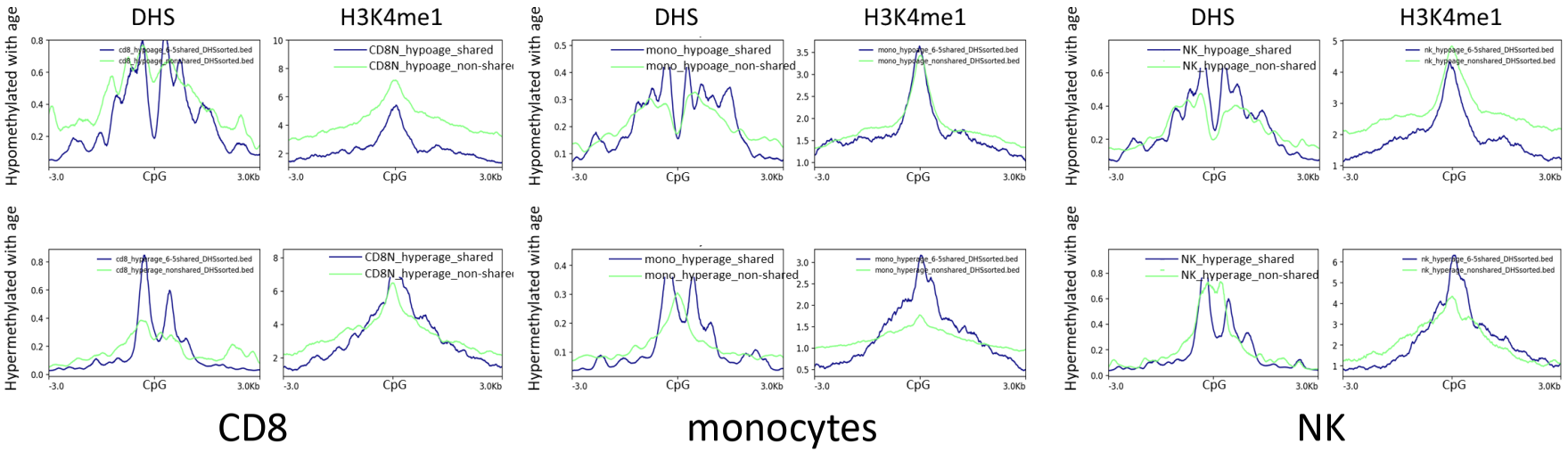

Roy et.al., Supp Figure 4

A.

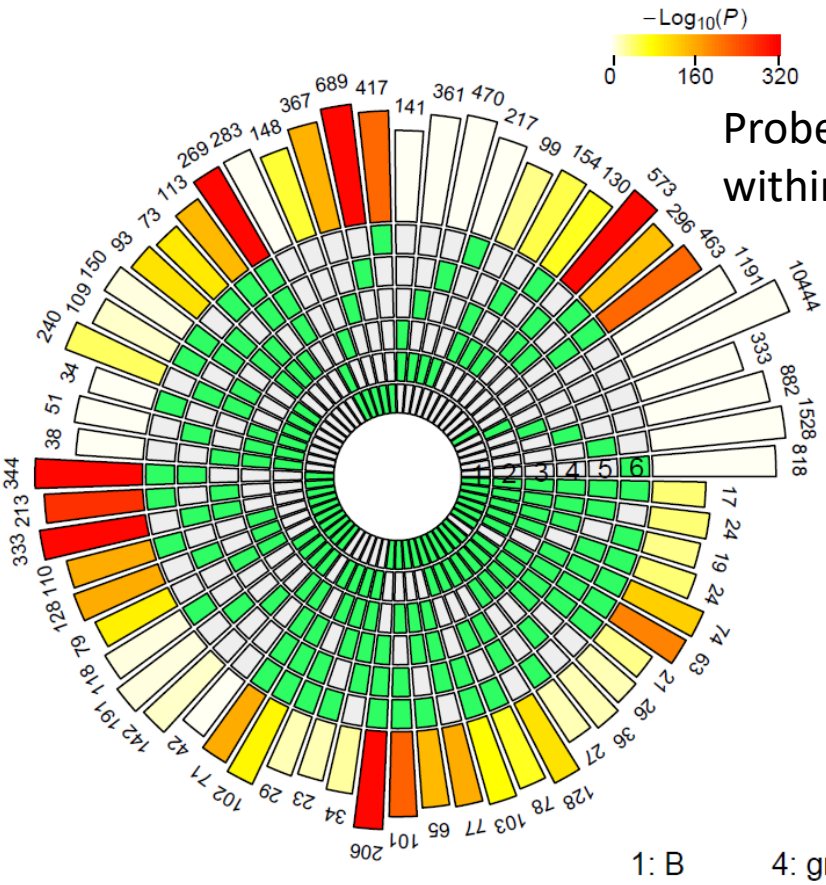
−Log10(P)
0
160
320
Probes with ARNT motif within 1kb
1: B
2: CD4
3: CD8
4: gran
5: mono
6: NK

B.

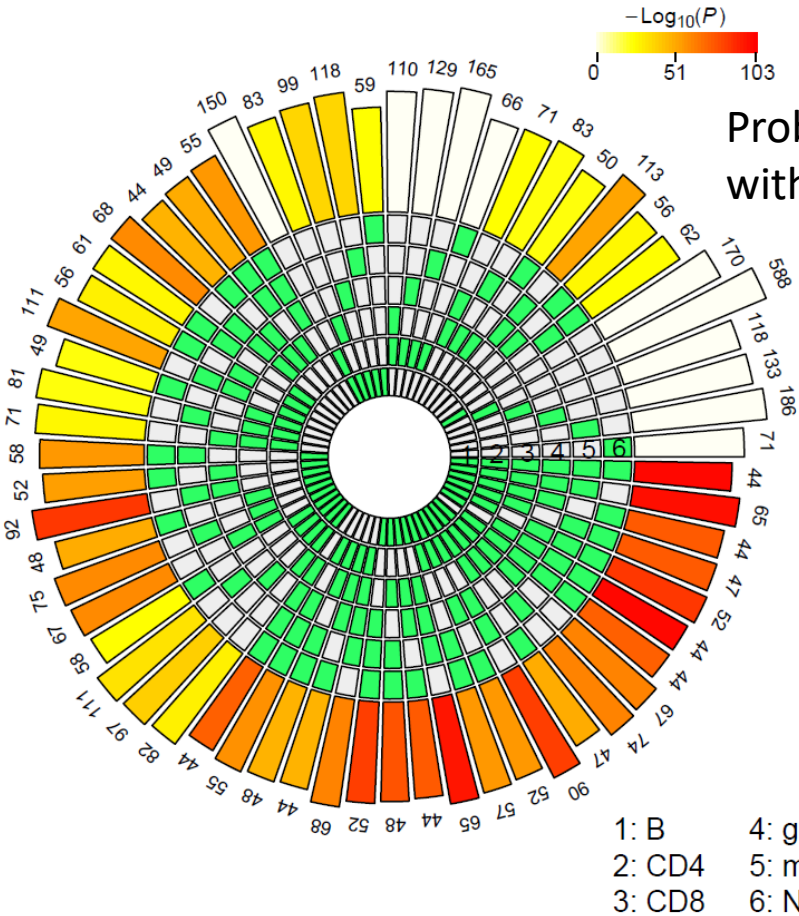
−Log10(P)
0
51
103
Probes with REST motif within 1kb
1: B
2: CD4
3: CD8
4: gran
5: mono
6: NK

Supplementary Table 1: Demographic and flow cytometry marker details of the cohort.

			Age groups							
Cell	Total	Males/Females	20s	30s	40s	50s	60s	70s	80s	Sorting markers
BN	49	31/18	8	7	5	7	9	10	3	$CD19^{+}CD27^{-}CD38^{+}$
CD4N	48	30/18	7	7	6	7	8	8	5	$CD4^{+}CD62L^{+}CD45RA^{+}$
CD8N	41	24/17	9	7	6	8	8	3	0	$CD8^{+}CD62L^{+}CD45RA^{+}$
Mono	52	32/20	8	7	6	8	9	8	6	$CD3^{-}CD91^{+}CD14^{+}$
NK	42	29/13	8	8	5	5	6	6	4	$CD3^{-}CD56^{+}CD16^{+}$
Granulo	40	24/16	8	6	4	4	4	8	6	Magnetic enrichment
PBMC	55	34/21	9	7	6	8	9	10	6	NA

Supplementary Table 2: Distribution of β-coefficient for probes significantly changing with age in the immune cells.

	BN		CD4N		CD8N		granulocytes		monocytes		NK	
β-coefficie	hypoage*	hyperage*	hypoage	hyperage	hypoage	hyperage	hypoage	hyperage	hypoage	hyperage	hypoage	hyperage
<0.01	5418	3558	63185	40787	1446	1576	4077	1211	7344	5186	3509	506
0.01-0.02	1018	287	321	274	379	122	525	116	824	211	609	109
0.02-0.03	63	17	56	21	24	5	24	4	46	14	28	7
>0.03	8	1	3	1	1	0	1	0	3	0	2	1
Total	6507	3863	63565	41083	1850	1703	4627	1331	8217	5411	4148	623

hypoage*- probes hypomethylated with age
hyperage*- probes hypermethylated with age

Supplementary Table 3: List of age-associated probes and their annotation for all the immune ce

ID	UCSC_Ref(	CHR	BP	location	padj	neglog_pa(	Group
cg1686765	ELOVL2	6	11044877	promoter	2.04E-30	29.69065	cd8n_hyperage
cg1686765	ELOVL2	6	11044877	promoter	4.04E-23	22.39319	mono_hyperage
cg1284126	LHFPL4	3	9594093	genebody	4.36E-22	21.36017	mono_hyperage
cg1062820	NFIA	1	61547131	genebody	5.14E-22	21.28892	nk_hypoage
cg0702456	THSD4	15	71615957	genebody	3.71E-21	20.43063	BN_hypoage
cg1686765	ELOVL2	6	11044877	promoter	8.12E-21	20.0906	nk_hyperage
cg1686765	ELOVL2	6	11044877	promoter	2.12E-20	19.67366	bn_hyperage
cg1355269	CCDC102B	18	66389447	promoter	4.73E-20	19.32479	cd8n_hypoage
cg2350053	0	5	1.4E+08	intergenic	5.56E-20	19.25457	mono_hyperage
cg2486641	LHFPL4	3	9594082	genebody	2.26E-19	18.64556	mono_hyperage
cg1686765	ELOVL2	6	11044877	promoter	4.93E-19	18.30692	gran_hyperage
cg2175726	FLT1	13	28896815	genebody	1.83E-18	17.73716	mono_hypoage
cg2157272	ELOVL2	6	11044894	promoter	1.83E-18	17.73716	mono_hyperage
cg1726865	FHL2	2	1.06E+08	promoter	2.64E-18	17.57795	nk_hyperage
cg1197034	GPR78	4	8582287	promoter	1.55E-17	16.80978	mono_hyperage
cg2005276	0	6	10510789	intergenic	1.57E-17	16.80543	nk_hypoage
cg2694703	0	7	33935438	intergenic	2.42E-17	16.61618	BN_hypoage
cg2157272	ELOVL2	6	11044894	promoter	2.77E-17	16.5569	cd8n_hyperage
cg1320672	GPR158	10	25463350	promoter	3.23E-17	16.49016	cd8n_hyperage
cg2255115	HMGA2	12	66342368	genebody	4.11E-17	16.38609	cd8n_hypoage
cg1364905	0	9	1.36E+08	intergenic	5.56E-17	16.25506	gran_hyperage
cg1355269	CCDC102B	18	66389447	promoter	1.9E-16	15.72125	BN_hypoage
cg0732348	EGFEM1P	3	1.68E+08	genebody	1.9E-16	15.7203	mono_hypoage
cg2157272	ELOVL2	6	11044894	promoter	1.95E-16	15.70932	gran_hyperage
cg2132364	0	22	31709724	intergenic	1.95E-16	15.70924	CD4N_hypoage
cg0649399	SCGN	6	25652602	promoter	3.14E-16	15.50334	mono_hyperage
cg1928380	CCDC102B	18	66389420	promoter	3.73E-16	15.42829	BN_hypoage
cg1284126	LHFPL4	3	9594093	genebody	3.83E-16	15.41673	gran_hyperage
cg0303249	0	14	61108227	intergenic	4.96E-16	15.30466	cd8n_hyperage
cg1355269	CCDC102B	18	66389447	promoter	8.63E-16	15.06393	mono_hypoage
cg1364905	0	9	1.36E+08	intergenic	1E-15	14.99906	mono_hyperage
cg2486641	LHFPL4	3	9594082	genebody	2.3E-15	14.63772	gran_hyperage
cg0708226	0	16	85429035	intergenic	2.33E-15	14.6329	mono_hypoage
cg0487512	OTUD7A	15	31775895	genebody	2.71E-15	14.56749	mono_hyperage
cg0176309	OTUD7A	15	31775406	genebody	4.54E-15	14.34281	nk_hyperage
cg2594019	NPAS3	14	33654069	genebody	4.69E-15	14.32853	nk_hypoage
cg1320672	GPR158	10	25463350	promoter	4.69E-15	14.32853	nk_hyperage
cg1317601	0	2	1.57E+08	intergenic	5.54E-15	14.25651	cd4n_hyperage
cg0754754	SLC12A5	20	44658225	genebody	7.55E-15	14.12198	mono_hyperage
cg1548036	CHGA	14	93389485	promoter	7.95E-15	14.0994	mono_hyperage
cg0732348	EGFEM1P	3	1.68E+08	genebody	9.28E-15	14.03245	BN_hypoage
cg1967112	CNGA3	2	98962974	promoter	1.14E-14	13.94248	mono_hyperage
cg1129954	PDCD1LG2	9	5510595	promoter	1.2E-14	13.92181	CD4N_hypoage
cg2703770	PRNT	20	4721316	promoter	1.2E-14	13.92181	CD4N_hypoage
cg1518110	0	1	21521531	intergenic	1.2E-14	13.92181	CD4N_hypoage

cg1967112	CNGA3	2	98962974	promoter	1.2E-14	13.92181	cd4n_hyperage
cg0702456	THSD4	15	71615957	genebody	2.14E-14	13.66969	mono_hypoage
cg0408096	EFNA5	5	1.07E+08	genebody	2.87E-14	13.54212	CD4N_hypoage
cg0162030	ADAM11	17	42856469	genebody	2.87E-14	13.54212	CD4N_hypoage
cg1355269	CCDC102B	18	66389447	promoter	2.87E-14	13.54212	CD4N_hypoage
cg1320672	GPR158	10	25463350	promoter	3.19E-14	13.49562	mono_hyperage
cg1726865	FHL2	2	1.06E+08	promoter	3.19E-14	13.49562	mono_hyperage
cg0649399	SCGN	6	25652602	promoter	3.28E-14	13.48386	nk_hyperage
cg2731555	NLGN1	3	1.73E+08	promoter	4.04E-14	13.39342	cd4n_hyperage
cg1329226	0	15	67238541	intergenic	4.04E-14	13.39342	CD4N_hypoage
cg1711058	0	19	36454623	intergenic	4.04E-14	13.39342	cd4n_hyperage
cg1467472	0	2	2.2E+08	intergenic	4.04E-14	13.39342	cd4n_hyperage
cg1364905	0	9	1.36E+08	intergenic	4.04E-14	13.39342	cd4n_hyperage
cg0163432	0	4	10162179	intergenic	4.17E-14	13.37986	BN_hypoage
cg2157272	ELOVL2	6	11044894	promoter	4.17E-14	13.37986	bn_hyperage
cg2095982	EBF1	5	1.59E+08	genebody	4.36E-14	13.36008	CD4N_hypoage
cg1380674	FAM181B	11	82443436	promoter	4.36E-14	13.36008	cd4n_hyperage
cg1729694	CNTN2	1	2.05E+08	genebody	4.51E-14	13.34573	CD4N_hypoage
cg1815569	LRP5	11	68214224	genebody	4.54E-14	13.34313	CD4N_hypoage
cg0863769	0	9	1.35E+08	intergenic	4.7E-14	13.32799	cd4n_hyperage
cg2078981	0	7	1.31E+08	intergenic	4.76E-14	13.32222	CD4N_hypoage
cg1077828	0	12	1.14E+08	intergenic	6.13E-14	13.21231	cd4n_hyperage
cg0691450	0	15	39464601	intergenic	7.03E-14	13.15278	mono_hypoage
cg1574983	VGLL4	3	11643341	genebody	7.44E-14	13.12816	cd4n_hyperage
cg1605427	F5	1	1.7E+08	promoter	7.44E-14	13.12816	CD4N_hypoage
cg2629485	TSPAN1	1	46645697	promoter	7.44E-14	13.12816	CD4N_hypoage
cg2541066	RPA2	1	28241577	promoter	7.44E-14	13.12816	cd4n_hyperage
cg2692196	0	5	92948217	intergenic	7.44E-14	13.12816	cd4n_hyperage
cg1207930	NFIA	1	61547163	genebody	8.51E-14	13.07007	BN_hypoage
cg1275701	TBR1	2	1.62E+08	genebody	8.62E-14	13.06433	cd4n_hyperage
cg0663932	FHL2	2	1.06E+08	promoter	9.15E-14	13.03862	mono_hyperage
cg2721793	LOC10013(	6	1.38E+08	genebody	9.38E-14	13.02796	cd4n_hyperage
cg0706055	SHANK1	19	51198381	genebody	9.39E-14	13.02727	cd4n_hyperage
cg0343191	0	17	77716367	intergenic	9.64E-14	13.01586	nk_hypoage
cg2654453	FLT1	13	28896826	genebody	1.03E-13	12.9859	mono_hypoage
cg0163432	0	4	10162179	intergenic	1.28E-13	12.89259	mono_hypoage
cg1240033	TJP1	15	30114871	promoter	1.36E-13	12.86624	cd4n_hyperage
cg0016354	B3GALT4	6	33246185	promoter	1.47E-13	12.83292	CD4N_hypoage
cg2279670	ARHGAP22	10	49673534	genebody	1.48E-13	12.82974	BN_hypoage
cg1038267	0	2	1.9E+08	intergenic	1.63E-13	12.78707	mono_hypoage
cg0036338	0	8	37641339	intergenic	1.64E-13	12.78553	CD4N_hypoage
cg1437792	MTA1	14	1.06E+08	genebody	1.67E-13	12.77827	CD4N_hypoage
cg1355269	CCDC102B	18	66389447	promoter	1.7E-13	12.76965	nk_hypoage
cg1994225	KCNA3	1	1.11E+08	promoter	1.78E-13	12.74934	CD4N_hypoage
cg2043789	0	2	2.2E+08	intergenic	1.78E-13	12.74934	CD4N_hypoage
cg0005922	GLRA1	5	1.51E+08	promoter	1.84E-13	12.73624	mono_hyperage
cg1623814	0	13	1.11E+08	intergenic	1.92E-13	12.7175	cd4n_hyperage

cg03776850		22	36461577	intergenic	1.97E-13	12.70469	mono_hypoage
cg0106507	TRAF3IP3	1	2.1E+08	promoter	2E-13	12.69818	CD4N_hypoage
cg1915468	GATAD2A	19	19600745	genebody	2E-13	12.69818	CD4N_hypoage
cg0648862	COL16A1	1	32131874	genebody	2E-13	12.69818	CD4N_hypoage
cg0355722	NPEPPS	17	45693418	genebody	2E-13	12.69818	CD4N_hypoage
cg24590480		12	13683399	intergenic	2E-13	12.69818	CD4N_hypoage
cg0931588	SYPL1	7	1.06E+08	promoter	2E-13	12.69818	CD4N_hypoage
cg1830470	MAST3	19	18229454	genebody	2E-13	12.69818	CD4N_hypoage
cg2001253	GPR123	10	1.35E+08	genebody	2E-13	12.69818	CD4N_hypoage
cg27209570		2	1.75E+08	intergenic	2E-13	12.69818	cd4n_hyperage
cg1169370	PAK6	15	40542019	promoter	2.21E-13	12.65561	BN_hypoage
cg1686765	ELOVL2	6	11044877	promoter	2.29E-13	12.64046	cd4n_hyperage
cg0809741	KLF14	7	1.3E+08	promoter	2.29E-13	12.64046	cd4n_hyperage
cg0495591	C2orf24	2	2.2E+08	genebody	2.33E-13	12.63213	CD4N_hypoage
cg1928380	CCDC102B	18	66389420	promoter	2.49E-13	12.60386	cd8n_hypoage
cg0755376	TRIM59	3	1.6E+08	promoter	2.8E-13	12.55348	cd8n_hyperage
cg11890720		7	1.51E+08	intergenic	2.96E-13	12.52921	CD4N_hypoage
cg26947030		7	33935438	intergenic	3.16E-13	12.50044	mono_hypoage
cg0809064	IFI35	17	41159289	genebody	3.25E-13	12.48766	CD4N_hypoage
cg1844842	APOL1	22	36648832	promoter	3.48E-13	12.45874	nk_hypoage
cg0505649	RCAN1	21	35899448	promoter	3.49E-13	12.45745	CD4N_hypoage
cg2629063	CALB1	8	91094847	promoter	3.54E-13	12.45038	cd4n_hyperage
cg21213070		10	30880636	intergenic	3.79E-13	12.42163	CD4N_hypoage
cg2153108	STPG1	1	24718669	genebody	3.97E-13	12.40137	mono_hypoage
cg1247648	UTRN	6	1.45E+08	genebody	4.03E-13	12.39502	cd4n_hyperage
cg0574311	WBP2	17	73850681	genebody	4.03E-13	12.39502	CD4N_hypoage
cg0958533	FAM89B	11	65340843	genebody	4.18E-13	12.37929	CD4N_hypoage
cg1484750	MAP3K8	10	30724194	promoter	4.18E-13	12.37929	cd4n_hyperage
cg14646980		9	34602974	intergenic	4.18E-13	12.37929	CD4N_hypoage
cg20786220		6	1.65E+08	intergenic	4.29E-13	12.36754	BN_hypoage
cg2245476	FHL2	2	1.06E+08	promoter	4.51E-13	12.34563	mono_hyperage
cg2002439	GLB1	3	33131138	genebody	4.63E-13	12.33412	CD4N_hypoage
cg18143290		3	1.58E+08	intergenic	4.71E-13	12.32681	cd4n_hyperage
cg1591367	TMEM105	17	79304420	promoter	4.76E-13	12.32239	CD4N_hypoage
cg2393321	PDE4DIP	1	1.45E+08	genebody	4.98E-13	12.30239	CD4N_hypoage
cg05770380		6	88722796	intergenic	5.06E-13	12.29593	CD4N_hypoage
cg19469500		20	49080681	intergenic	5.06E-13	12.29593	CD4N_hypoage
cg0708037	SLC25A22	11	796607	promoter	5.06E-13	12.29593	CD4N_hypoage
cg24049880		10	1.03E+08	intergenic	5.13E-13	12.29008	CD4N_hypoage
cg0660284	DBC1	9	1.22E+08	promoter	5.15E-13	12.28824	cd4n_hyperage
cg0740845	PGLYRP2	19	15590532	promoter	5.85E-13	12.23287	mono_hypoage
cg02383780		7	1.28E+08	intergenic	6.05E-13	12.21836	cd4n_hyperage
cg1985547	CACNA1I	22	40060836	genebody	6.11E-13	12.21387	cd4n_hyperage
cg23756170		17	26577713	intergenic	6.68E-13	12.17523	cd4n_hyperage
cg2332310	EHD1	11	64643272	genebody	6.86E-13	12.16345	CD4N_hypoage
cg24970170		14	77339984	intergenic	6.86E-13	12.16345	CD4N_hypoage
cg1765647	IQSEC3	12	176424	promoter	6.86E-13	12.16345	cd4n_hyperage

cg2336871	C1R	12	7245510	promoter	7.02E-13	12.15368	CD4N_hypoage
cg0754754	SLC12A5	20	44658225	genebody	7.02E-13	12.15368	cd4n_hyperage
cg1551713	CTLA4	2	2.05E+08	genebody	7.16E-13	12.14537	CD4N_hypoage
cg1491264	0	2	1.57E+08	intergenic	7.16E-13	12.14537	cd4n_hyperage
cg0694818	FAM219A	9	34403522	genebody	8.02E-13	12.0956	CD4N_hypoage
cg1082748	ZBTB16	11	1.14E+08	genebody	8.02E-13	12.0956	cd4n_hyperage
cg2194311	0	1	2840308	intergenic	8.02E-13	12.0956	CD4N_hypoage
cg0175294	0	2	1.1E+08	intergenic	8.02E-13	12.0956	CD4N_hypoage
cg2330464	GNA12	7	2778058	genebody	8.24E-13	12.08416	cd4n_hyperage
cg1795678	0	22	30649441	intergenic	8.68E-13	12.06161	cd4n_hyperage
cg2558058	0	10	3853668	intergenic	8.8E-13	12.05552	CD4N_hypoage
cg0944343	AUTS2	7	69126948	genebody	9.31E-13	12.03127	CD4N_hypoage
cg2473275	IFRD2	3	50330513	promoter	9.31E-13	12.03127	CD4N_hypoage
cg2246336	AKNA	9	1.17E+08	genebody	9.34E-13	12.02951	cd4n_hyperage
cg0234906	RNASEL	1	1.83E+08	promoter	9.34E-13	12.02951	CD4N_hypoage
cg2319879	CAPN3	15	42694406	genebody	9.69E-13	12.01369	cd4n_hyperage
cg1971577	CBX4	17	77810912	genebody	9.81E-13	12.00813	cd4n_hyperage
cg1711058	0	19	36454623	intergenic	9.93E-13	12.00315	mono_hyperage
cg1637717	STAT5B	17	40392955	promoter	9.95E-13	12.00208	cd4n_hyperage
cg2302758	CRH	8	67089513	genebody	9.95E-13	12.00208	cd4n_hyperage
cg0422905	SLC38A7	16	58718971	promoter	9.95E-13	12.00208	CD4N_hypoage
cg0663932	FHL2	2	1.06E+08	promoter	1.04E-12	11.98297	bn_hyperage
cg1289230	C17orf104	17	42733592	promoter	1.04E-12	11.98125	nk_hyperage
cg1042497	0	16	66388348	intergenic	1.36E-12	11.8663	mono_hypoage
cg0974874	ASL	7	65540429	promoter	1.36E-12	11.8663	mono_hypoage
cg0364878	NRM	6	30659345	promoter	1.47E-12	11.83207	mono_hypoage
cg0750461	0	3	14832729	intergenic	1.47E-12	11.83207	mono_hypoage
cg0823450	0	5	1.39E+08	intergenic	2.1E-12	11.67821	mono_hypoage
cg1820469	NOX3	6	1.56E+08	genebody	2.26E-12	11.64595	mono_hypoage
cg2692464	C11orf49	11	47026076	genebody	2.57E-12	11.59007	mono_hypoage
cg1217991	0	12	22568845	intergenic	3.44E-12	11.46344	BN_hypoage
cg0549868	0	7	7142996	intergenic	3.64E-12	11.4389	BN_hypoage
cg0708226	0	16	85429035	intergenic	4.09E-12	11.38839	nk_hypoage
cg1174120	FJX1	11	35638398	promoter	4.27E-12	11.36957	BN_hypoage
cg0152854	0	12	81468232	intergenic	4.42E-12	11.35491	mono_hypoage
cg0231878	0	15	27213174	intergenic	4.43E-12	11.35386	mono_hyperage
cg0026692	ST8SIA3	18	55021277	genebody	4.43E-12	11.35319	mono_hyperage
cg0791461	0	1	62072468	intergenic	4.44E-12	11.35267	nk_hypoage
cg0678499	ZYG11A	1	53308768	genebody	4.49E-12	11.34817	mono_hyperage
cg1856849	SLC2A13	12	40406687	genebody	4.54E-12	11.34294	BN_hypoage
cg2255115	HMGA2	12	66342368	genebody	4.54E-12	11.34294	BN_hypoage
cg1671476	DCHS2	4	1.55E+08	genebody	4.72E-12	11.32587	nk_hypoage
cg0708226	0	16	85429035	intergenic	4.95E-12	11.30539	BN_hypoage
cg2723697	KRT17	17	39781997	promoter	4.95E-12	11.30539	BN_hypoage
cg0809741	KLF14	7	1.3E+08	promoter	5.56E-12	11.25457	mono_hyperage
cg1638116	0	21	16031542	intergenic	5.68E-12	11.24545	mono_hypoage
cg0303249	0	14	61108227	intergenic	5.77E-12	11.23894	nk_hyperage

cg2059545	VPS52	6	33219392	genebody	5.95E-12	11.22548	BN_hypoage
cg1941957	SP1	12	53808961	genebody	6.03E-12	11.21968	mono_hypoage
cg1108433	LHFPL4	3	9594264	genebody	6.03E-12	11.21968	mono_hyperage
cg2594019	NPAS3	14	33654069	genebody	6.67E-12	11.17587	BN_hypoage
cg1305330	MAP1B	5	71435267	genebody	6.67E-12	11.17587	BN_hypoage
cg2078622	0	6	1.65E+08	intergenic	7.03E-12	11.15285	nk_hypoage
cg1536684	0	4	6012468	intergenic	7.03E-12	11.15285	nk_hypoage
cg0663932	FHL2	2	1.06E+08	promoter	7.03E-12	11.15285	nk_hyperage
cg2694703	0	7	33935438	intergenic	7.7E-12	11.11375	cd8n_hypoage
cg0215151	0	9	35955041	intergenic	7.97E-12	11.0983	mono_hypoage
cg2553324	AKAP8L	19	15530630	promoter	8.41E-12	11.0752	BN_hypoage
cg2542788	0	10	1.02E+08	intergenic	9.79E-12	11.0093	mono_hyperage
cg0972793	LINC00577	6	1.05E+08	promoter	9.91E-12	11.00406	mono_hyperage
cg0033133	0	4	1.56E+08	intergenic	1.04E-11	10.98369	mono_hypoage
cg0702456	THSD4	15	71615957	genebody	1.06E-11	10.97267	nk_hypoage
cg2374649	0	6	1.05E+08	intergenic	1.11E-11	10.95652	mono_hyperage
cg1534112	DIO3	14	1.02E+08	promoter	1.19E-11	10.92365	mono_hyperage
cg2594019	NPAS3	14	33654069	genebody	1.36E-11	10.86501	mono_hypoage
cg0980967	EDARADD	1	2.37E+08	promoter	1.38E-11	10.8614	nk_hypoage
cg1976127	CSNK1D	17	80232096	promoter	1.39E-11	10.85735	cd8n_hypoage
cg2542788	0	10	1.02E+08	intergenic	1.57E-11	10.8041	bn_hyperage
cg0541202	ABCC4	13	95952937	genebody	1.69E-11	10.77211	BN_hypoage
cg0802368	0	10	1.21E+08	intergenic	1.7E-11	10.76955	BN_hypoage
cg0569402	0	12	19699504	intergenic	1.7E-11	10.76955	BN_hypoage
cg1638116	0	21	16031542	intergenic	1.7E-11	10.76955	BN_hypoage
cg1393122	MPP6	7	24612418	promoter	1.7E-11	10.76955	BN_hypoage
cg2641350	0	6	1.41E+08	intergenic	1.78E-11	10.74838	mono_hypoage
cg1928380	CCDC102B	18	66389420	promoter	1.98E-11	10.70267	mono_hypoage
cg0176309	OTUD7A	15	31775406	genebody	1.98E-11	10.70267	mono_hyperage
cg0754418	CILP2	19	19651235	genebody	2.02E-11	10.69465	bn_hyperage
cg1355269	CCDC102B	18	66389447	promoter	2.23E-11	10.65265	gran_hypoage
cg0705757	0	15	95870112	intergenic	2.3E-11	10.63861	mono_hyperage
cg1934462	NWD1	19	16830749	promoter	2.31E-11	10.63613	nk_hypoage
cg1305330	MAP1B	5	71435267	genebody	2.4E-11	10.62027	mono_hypoage
cg2245476	FHL2	2	1.06E+08	promoter	2.52E-11	10.59791	nk_hyperage
cg2010529	0	5	1.51E+08	intergenic	2.6E-11	10.58514	mono_hypoage
cg0599145	0	4	1.48E+08	intergenic	2.71E-11	10.56774	mono_hyperage
cg2548537	0	4	1.06E+08	intergenic	2.75E-11	10.56067	BN_hypoage
cg1289327	FLT1	13	28922440	genebody	3.2E-11	10.49454	mono_hypoage
cg1169370	PAK6	15	40542019	promoter	3.41E-11	10.46682	cd8n_hypoage
cg2294700	BCMO1	16	81272281	promoter	3.43E-11	10.46471	BN_hypoage
cg1364905	0	9	1.36E+08	intergenic	3.43E-11	10.46471	bn_hyperage
cg1050121	0	1	2.08E+08	intergenic	3.55E-11	10.45031	mono_hypoage
cg1000118	0	11	94882829	intergenic	3.55E-11	10.45031	mono_hypoage
cg1466783	ALK	2	30064491	genebody	3.57E-11	10.44733	BN_hypoage
cg0377685	0	22	36461577	intergenic	3.57E-11	10.44733	BN_hypoage
cg1221169	ADGRB2	1	32211779	genebody	3.71E-11	10.43012	mono_hypoage

cg0541202	ABCC4	13	95952937	genebody	3.78E-11	10.42269	cd8n_hypoage
cg0980967	EDARADD	1	2.37E+08	promoter	3.78E-11	10.42269	cd8n_hypoage
cg1976127	CSNK1D	17	80232096	promoter	3.81E-11	10.4193	mono_hypoage
cg2116508	C11orf85	11	64739736	promoter	3.81E-11	10.4193	mono_hyperage
cg0755376	TRIM59	3	1.6E+08	promoter	4.07E-11	10.39086	mono_hyperage
cg0458193	0	6	31364999	intergenic	4.39E-11	10.35754	BN_hypoage
cg1820469	NOX3	6	1.56E+08	genebody	4.39E-11	10.35754	BN_hypoage
cg0755376	TRIM59	3	1.6E+08	promoter	4.39E-11	10.35754	bn_hyperage
cg1285788	0	17	29911146	intergenic	4.84E-11	10.31515	BN_hypoage
cg0740845	PGLYRP2	19	15590532	promoter	4.84E-11	10.31515	BN_hypoage
cg0662319	MTMR3	22	30400763	genebody	4.84E-11	10.31515	BN_hypoage
cg1580921	BAT3	6	31607648	genebody	4.84E-11	10.31515	BN_hypoage
cg2641350	0	6	1.41E+08	intergenic	4.84E-11	10.31515	BN_hypoage
cg2245476	FHL2	2	1.06E+08	promoter	4.84E-11	10.31515	bn_hyperage
cg0343191	0	17	77716367	intergenic	4.94E-11	10.30603	mono_hypoage
cg2175726	FLT1	13	28896815	genebody	5.19E-11	10.28483	BN_hypoage
cg1864524	0	21	43022102	intergenic	5.19E-11	10.28483	BN_hypoage
cg2024956	NWD1	19	16830739	promoter	5.21E-11	10.28355	nk_hypoage
cg0646732	0	9	1.03E+08	intergenic	5.44E-11	10.2644	BN_hypoage
cg1693282	0	3	1.94E+08	intergenic	5.46E-11	10.26261	mono_hypoage
cg1788522	0	6	1.05E+08	intergenic	5.46E-11	10.26261	mono_hyperage
cg0373802	0	6	1.05E+08	intergenic	5.56E-11	10.25475	mono_hyperage
cg0791461	0	1	62072468	intergenic	5.62E-11	10.25026	BN_hypoage
cg0487512	OTUD7A	15	31775895	genebody	6.18E-11	10.20877	nk_hyperage
cg1726865	FHL2	2	1.06E+08	promoter	6.3E-11	10.20066	bn_hyperage
cg1320806	NWD1	19	16830563	promoter	6.37E-11	10.19559	cd8n_hypoage
cg0319304	0	4	74570180	intergenic	6.48E-11	10.18867	nk_hypoage
cg0408415	VGF	7	1.01E+08	promoter	6.49E-11	10.18768	nk_hyperage
cg1207930	NFIA	1	61547163	genebody	6.63E-11	10.17845	nk_hypoage
cg2663871	NRXN3	14	80053724	genebody	6.82E-11	10.16622	BN_hypoage
cg1934462	NWD1	19	16830749	promoter	6.82E-11	10.16622	BN_hypoage
cg1548036	CHGA	14	93389485	promoter	7.23E-11	10.1408	gran_hyperage
cg0149947	COL4A2	13	1.11E+08	genebody	7.39E-11	10.13136	BN_hypoage
cg2005276	0	6	10510789	intergenic	7.39E-11	10.13136	BN_hypoage
cg1928380	CCDC102B	18	66389420	promoter	7.46E-11	10.12732	nk_hypoage
cg2641350	0	6	1.41E+08	intergenic	7.46E-11	10.12732	nk_hypoage
cg1902858	0	5	1.43E+08	intergenic	7.8E-11	10.10791	BN_hypoage
cg1062820	NFIA	1	61547131	genebody	7.87E-11	10.10403	BN_hypoage
cg1641923	PENK	8	57360613	promoter	7.96E-11	10.09934	mono_hyperage
cg1600896	0	1	1.15E+08	intergenic	8.29E-11	10.08145	BN_hypoage
cg0185554	DUSP16	12	12716653	promoter	8.63E-11	10.06399	BN_hypoage
cg1743869	0	1	1.87E+08	intergenic	8.94E-11	10.04875	nk_hypoage
cg1235047	0	17	46578476	intergenic	9.8E-11	10.00879	nk_hypoage

Supplementary Table 4- Top 15 age-hypo and hypermethylated genes in each cell type

	BN	CD4N	CD8N	monocytes	NK	granulocytes
genes hypomethylated with age	**THSD4**	PDCD1LG2	**CCDC102B**	FLT1	**NFIA**	**CCDC102B**
	CCDC102B	PRNT	**HMGA2**	**EGFEM1P**	**NPAS3**	SEMA7A
	EGFEM1P	EFNA5	CSNK1D	**CCDC102B**	**CCDC102B**	IL21R
	NFIA	ADAM11	**PAK6**	**THSD4**	APOL1	LAG3
	ARHGAP22	**CCDC102B**	**ABCC4**	STPG1	DCHS2	LMNA
	PAK6	EBF1	**EDARADD**	PGLYRP2	THSD4	PDCD1LG2
	FJX1	**CNTN2**	NWD1	ASL	**EDARADD**	SLC25A22
	SLC2A13	LRP5	PDE1C	NRM	NWD1	STPG1
	HMGA2	F5	**THSD4**	NOX3	ACSS3	**THSD4**
	KRT17	TSPAN1	HLA-DPB1	**C11orf49**	ASPA	LDB2
	VPS52	B3GALT4	**MAP1B**	SP1	P3H2	SAMD14
	NPAS3	MTA1	**NPAS3**	**NPAS3**	FLJ23834	**C11orf49**
	MAP1B	KCNA3	PI4KB	MAP1B	SIGIRR	DNER
	AKAP8L	TRAF3IP3	EIF1	ADGRB2	PTGDS	STOML1
	ABCC4	GATAD2A	**CNTN4**	CSNK1D	RNF182	RARRES3
	genes observed in more than 1 cell type					

	BN	CD4N	CD8N	monocytes	NK	granulocytes
genes hypermethylated with age	**ELOVL2**	**CNGA3**	**ELOVL2**	**ELOVL2**	**ELOVL2**	**ELOVL2**
	FHL2	NLGN1	**GPR158**	**LHFPL4**	**FHL2**	**LHFPL4**
	CILP2	FAM181B	**TRIM59**	**GPR78**	**OTUD7A**	**CHGA**
	TRIM59	VGLL4	RPA2	**SCGN**	**GPR158**	SOBP
	LHFPL4	RPA2	ALDH1A2	**OTUD7A**	**SCGN**	**GPR158**
	STXBP5L	TBR1	**KLF14**	**SLC12A5**	C17orf104	PRRT4
	CHGA	LOC100130476	**GPR62**	CHGA	VGF	**KLF14**
	GPR78	SHANK1	SYNGR3	**CNGA3**	**GPR176**	**SLC12A5**
	OTUD7A	TJP1	ALX3	**GPR158**	**CHGA**	DIO3
	GPR158	**ELOVL2**	**LHFPL4**	**FHL2**	NXPH1	BOK
	PC	**KLF14**	LRP5	GLRA1	**LHFPL4**	SCGN
	NEFM	CALB1	SP8	ST8SIA3	TRIM59	SYT14
	VGF	UTRN	ADCY5	ZYG11A	CALB1	PRLHR
	AFAP1	MAP3K8	FHL2	**KLF14**	**KLF14**	NXPH1
	KLF14	DBC1	PPM1E	LINC00577	PENK	GLRA1
	genes observed in more than 1 cell type					

Supplementary Table 5: Detailed Gene Set Enrichment Analysis Output

Gene_Set	Group	ID	Pathway	b	B	n	N	E	p_Val	q_Val	Genes_in_Pathway
Hallmarks	common_hyper	M5957	Hallmark pancreas beta cells	6	40	226	26325	17.47	#####	#####	PAX6,NEUROD1,PCSK1,SCGN,CHGA,SST
Reactome	common_hyper	M735	Reactome neuronal system	17	409	225	25982	4.8	#####	2E-04	SYT7,RIMS1,KCNA7,SLC6A4,KCNC4,GRIA2,KCNS1,KCNC3,SLC6A3,GLRA1,CACNA1B,SHANK1,KCNC2,CACNG2,ADCY5,PPM1E,GRIN1
KEGG	common_hyper	M13380	Kegg neuroactive ligand receptor interaction	11	269	226	26361	4.77	#####	0.004	ADRB1,DRD2,SSTR2,PRLHR,NTSR2,GRIA2,HTR6,HTR7,AVPR1A,GLRA1,GRIN1
Reactome	common_hypo	M41809	Reactome rac1 gtpase cycle	13	184	426	25982	4.309	#####	0.007	PLEKHG6,NISCH,RAB7A,GIT1,MCF2L,DOCK4,ARHGAP22,PLD2,PAK6,ARHGAP17,KALRN,DLC1,ARHGAP12
Reactome	common_hypo	M26999	Reactome collagen biosynthesis and modifying enzymes	8	67	426	25982	7.282	#####	0.007	P3H2,COL1A1,COL6A1,ADAMTS3,COL6A3,COL22A1,COL8A2,COL15A1
Reactome	common_hypo	M27078	Reactome rho gtpase cycle	21	443	426	25982	2.891	#####	0.007	PLEKHG6,NISCH,ARHGEF10L,RAB7A,STMN2,GIT1,CCDC88A,MCF2L,DOCK4,NDUFA5,ARHGAP22,PLD2,PAK6,ARHGAP17,CDC42EP2,PLEKHG4B,KALRN,DLC1,ARHGAP12,KCTD13,SPTAN1
Reactome	common_hypo	M631	Reactome collagen formation	9	90	426	25982	6.099	#####	0.007	P3H2,COL1A1,LOXL4,COL6A1,ADAMTS3,COL6A3,COL22A1,COL8A2,COL15A1
KEGG	common_hypo	M16476	Kegg cell adhesion molecules cams	10	130	426	26361	4.76	#####	0.01	CD274,PDCD1LG2,CD4,NRXN3,HLA-DPB1,HLA-C,HLA-B,PTPRF,CNTNAP2,CNTN2
KEGG	common_hyper	M2890	Kegg calcium signaling pathway	8	176	226	26361	5.302	1E-04	0.014	ADRB1,GRIN1,CACNA1B,HTR6,HTR7,AVPR1A,CACNA1G,CACNA1I
Reactome	common_hypo	M19752	Reactome complement cascade	7	58	426	25982	7.361	#####	0.014	CLU,MASP1,C5AR2,C1QC,C1R,C3AR1,CR1
WP	common_hyper	M39891	Wp genes controlling nephrogenesis	5	43	226	26124	13.44	#####	0.016	FGF8,GDNF,HOXD11,NPHS1,GLI3
WP	common_hyper	M39607	Wp tgif disruption of shh signaling	3	9	226	26124	38.53	#####	0.016	FOXG1,FGF8,GLI3
WP	common_hyper	M39373	Wp sudden infant death syndrome sids susceptibility pathways	8	162	226	26124	5.708	#####	0.018	SST,SSTR2,TP73,PHOX2B,SLC6A4,NEUROD1,GRIN1,TAC1
Reactome	common_hypo	M27812	Reactome collagen chain trimerization	6	44	426	25982	8.317	#####	0.021	COL1A1,COL6A1,COL6A3,COL22A1,COL8A2,COL15A1
Reactome	common_hyper	M1056	Reactome voltage gated potassium channels	5	43	225	25982	13.43	#####	0.021	KCNA7,KCNC4,KCNS1,KCNC3,KCNC2

Reactome	common_hyper	M746	Reactome signaling by gpcr	18	696	225	25982	2.986	#####	0.021	TAC1,ADRB1,PDE4C,PRLHR,RGS22,WNT2B,HTR7,DRD2,OBSCN,SST,HTR6,GPR176,AVPR1A,NTSR2,GPR25,ADCY5,SSTR2,PENK
Hallmarks	common_hypo	M5909	Hallmark myogenesis	11	200	427	26325	3.391	5E-04	0.023	TNNT3,MYL3,COL15A1,COL6A3,NAV2,CLU,COL1A1,NQO1,SPTAN1,ABLIM1,APP
Hallmarks	common_hypo	M5902	Hallmark apoptosis	9	161	427	26325	3.446	0.001	0.026	SPTAN1,PDGFRB,TSPO,CLU,LMNA,ENO2,APP,SOD2,BMP2
Hallmarks	common_hypo	M5893	Hallmark mitotic spindle	10	198	427	26325	3.114	0.002	0.026	NUMA1,KIF5B,CDC42EP2,CCDC88A,DOCK4,CENPE,KIF3C,SPTAN1,PXN,CSNK1D
WP	common_hypo	M39649	Wp complement and coagulation cascades	7	58	426	26124	7.401	#####	0.026	F5,CR1,C1QC,C1R,C3AR1,CLU,MASP1
WP	common_hyper	M39585	Wp monoamine gpcrs	4	33	226	26124	14.01	2E-04	0.028	HTR7,HTR6,ADRB1,DRD2
Reactome	common_hyper	M27120	Reactome thyroxine biosynthesis	3	10	225	25982	34.64	#####	0.029	DUOX1,DUOX2,DIO3
WP	common_hyper	M39575	Wp ectoderm differentiation	7	142	226	26124	5.698	2E-04	0.03	FHL2,SIX6,ELOVL2,CLVS1,GLI3,NR2F2,PAX6
Hallmarks	common_hypo	M5942	Hallmark uv response dn	8	144	427	26325	3.425	0.002	0.031	ABCC1,MAP1B,KCNMA1,NRP1,COL1A1,PDGFRB,KALRN,DLC1
PID	common_hypo	M160	Pid avb3 integrin pathway	7	74	427	26458	5.861	2E-04	0.038	PXN,PI4KB,COL8A2,COL6A3,COL6A1,COL15A1,COL1A1
Reactome	common_hyper	M15514	Reactome transmission across chemical synapses	10	268	225	25982	4.309	1E-04	0.039	RIMS1,SLC6A4,GRIA2,SLC6A3,GLRA1,CACNA1B,CACNG2,ADCY5,PPM1E,GRIN1
Reactome	common_hyper	M18334	Reactome class a 1 rhodopsin like receptors	11	329	225	25982	3.861	2E-04	0.039	TAC1,ADRB1,PRLHR,HTR7,DRD2,SST,HTR6,AVPR1A,NTSR2,SSTR2,PENK
Reactome	common_hyper	M27318	Reactome synthesis secretion and inactivation of glucose dependent insulinotropic polypeptide gip	3	13	225	25982	26.65	2E-04	0.039	PAX6,GATA4,PCSK1
Hallmarks	common_hypo	M5930	Hallmark epithelial mesenchymal transition	9	199	427	26325	2.788	0.005	0.046	FBN1,COL1A1,COL6A3,TPM1,SLIT3,COL8A2,SCG2,ENO2,PDGFRB
Hallmarks	common_hypo	M5921	Hallmark complement	9	200	427	26325	2.774	0.006	0.046	C1R,F5,C1QC,CR1,CLU,ZFPM2,SH2B3,L3MBTL4,DOCK4

INDEX

b	number of genes from input list significantly associated with the particular pathway
B	number of genes from background list(all EPIC probes) significantly associated with the particular pathway
n	total number of genes from input list associated with the particular pathway
N	total number of genes from background list(all EPIC probes) associated with the particular pathway
E	enrichment score
p_Val	enrichment p value
q_Val	enrichment adjusted q value

Supplementary Table 6: Age-associated differences of transcripts for ARNT, REST and CTCF.

	BN	CD4N	CD8N	granulocyt	monocytes	NK
ARNT	$<10^{-11}$	$<10^{-11}$	$<10^{-11}$	$<10^{-11}$	$<10^{-11}$	$<10^{-11}$
CTCF	$<10^{-11}$	$<10^{-11}$	$<10^{-11}$	$<10^{-10}$	$<10^{-11}$	$<10^{-11}$
REST	0.05	<0.001	N.S.	$<10^{-7}$	<0.01	<0.05

Cyan- negative relationship between gene expression and age

Magenta- positive relationship between gene expression and age

*unadjusted p-values from linear regression